

Wet Clutch Tribotesting

Friction Assessment for Shudder Tendency Evaluation Routine

Erik Nyberg
2015

Master of Science in Engineering Technology
Mechanical Engineering

Luleå University of Technology
Department of Engineering Sciences and Mathematics

Preface

This master's thesis has been conducted at the Division of Machine Elements, Luleå University of Technology, in cooperation with BorgWarner TorqTransfer Systems in Landskrona. I would like to thank all the people involved in this project, Pär Marklund and Kim Berglund at Machine Elements, LTU, and Jonas Jönsson and Richard Olsson at BorgWarner.

*Erik Nyberg,
June 2015, Luleå*

Page intentionally left blank

Abstract

Modern all-wheel drive systems require accurate torque transfer during the entire lifetime of the system. In order to provide this, the friction coefficient must be predicted. The friction depends heavily on factors such as temperature and sliding speed in the friction interface, but it is also affected by ageing of the system and especially oxidation of the lubricant. Component test rigs are often used to evaluate ageing of wet clutch systems. However, these tests are time consuming and often involve many parameters which are difficult to control. Model scale testing on the other hand is quick and provides good control of test parameters, but require more interpretation of how the test results relate to the real application.

In this master's thesis work, a quick routine for analyzing and processing model scale test data from pin-on-disc experiments has been developed, in combination with a one degree-of-freedom dynamic model of a component test rig. The routine assesses the friction characteristics of a wet clutch system consisting of clutch disc materials and lubricants, and predicts if the investigated material and lubricant combination is likely to induce shudder in the wet clutch component test rig.

The developed routine is well suited for screening experiments of new lubricants or materials as the data processing is generalized and capable of representing any material and lubricant combination in the simulation. Using this routine with an artificial oil ageing method could possibly be a very efficient complement to component scale testing.

Page intentionally left blank

NOMENCLATURE	1
<hr/>	
1 INTRODUCTION	3
1.1 BACKGROUND OF AWD-SYSTEMS	3
1.2 WET CLUTCHES IN AWD	4
1.3 EFFECTS OF AGEING	5
1.4 CURRENT STATE	5
1.5 OBJECTIVES	6
2 WET CLUTCH THEORY	7
<hr/>	
2.1 WET CLUTCH OPERATING CONDITIONS	7
2.1.1 BOUNDARY LUBRICATION AND TRIBOFILM FORMATION	8
2.2 WET CLUTCH COMPONENTS	9
2.2.1 CLUTCH DISCS	9
2.2.2 LUBRICANTS	10
2.3 TRIBOLOGICAL FAILURES IN WET CLUTCHES	12
2.3.1 SURFACE FAILURE	13
2.3.2 LUBRICANT FAILURE	13
2.4 WET CLUTCH DYNAMICS	15
2.4.1 ROTATIONAL MECHANICAL SYSTEM	16
2.4.2 THERMODYNAMICS	17
2.4.3 STICK-SLIP AND SHUDDER PHENOMENA	17
3 MATERIALS AND TEST EQUIPMENT	21
<hr/>	
3.1 MATERIALS IN FRICTION INTERFACE	21
3.2 PIN-ON-DISC EQUIPMENT	22
3.3 WET CLUTCH TEST RIG	23
3.4 AUXILIARY EQUIPMENT	24
4 PART I – FRICTION ASSESSMENT FOR SHUDDER TENDENCY EVALUATION ROUTINE (FASTER)	25
<hr/>	
4.1 FRICTION ASSESSMENT BY PIN-ON-DISC	25
4.1.1 POD EXPERIMENTAL PROCEDURE	25
4.1.2 POD DATA ANALYSIS	27
4.2 DYNAMIC SIMULATION OF WET CLUTCH TEST RIG	31
5 PART II – DEMONSTRATION OF FASTER	35
<hr/>	
5.1 VALIDATION OF FASTER	35
5.1.1 ESTABLISHING SHUDDER LIMIT IN WET CLUTCH TEST RIG	35
5.1.2 ANALYSIS OF SHUDDER LIMIT OIL BY FASTER	37
5.2 EVALUATION OF DEGRADED OIL BY FASTER	37

5.2.1	THERMAL AGEING OF OIL SAMPLES	37
5.2.2	OIL DEGRADATION BY WATER CONTAMINATION	38
6	RESULTS & DISCUSSION	39
6.1	RESULTS VALIDATING FASTER	39
6.1.1	PREDICTION OF FASTER	39
6.1.2	ESTABLISHED SHUDDER LIMIT IN WCTR	44
6.2	FACTORS INFLUENCING ACCURACY OF FASTER	45
6.2.1	EFFECT OF ALIGNING AND CONDITION OF PIN SPECIMEN	45
6.2.2	EFFECT OF BIN DISTRIBUTION	47
6.3	FASTER PREDICTION FOR AGED AND DEGRADED OIL	48
7	CONCLUSIONS	53
8	FUTURE WORK	55
9	REFERENCES	57
APPENDIX		I
	MATLAB CODE – FAST IMPORTER	I
	MATLAB CODE – FAST EVALUATOR	I
	MATLAB CODE – INPUTS TO DYNAMIC MODEL	I
	SIMULINK DYNAMIC MODEL	I

Nomenclature

τ_T	Transferred torque	[Nm]
μ	Friction coefficient	[-]
F_{ax}	Axial force	[N]
R_f	Mean friction radius	[m]
N_{int}	Number of interfaces	[-]
Λ	Film parameter	[-]
R_{qA}	RMS roughness of surface A	[m]
R_{qB}	RMS roughness of surface B	[m]
H	Hersey number	[-]
h	Film thickness	[m]
η	Viscosity	[Pa · s]
p	Pressure	[Pa]
v	Sliding speed	[m/s]
α_m	Share of metal contact	[-]
μ_m	Friction coefficient for metal contact	[-]
μ_1	Friction coefficient for tribofilm contact	[-]
α	Depletion state of friction modifying additives	[-]
μ_d	Friction coefficient for wet clutch system with additive depleted oil	[-]
μ_f	Friction coefficient for wet clutch system with fully formulated oil	[-]
RH	Hydrocarbon chain	[-]
$R \bullet$	Alkyl radical	[-]
$H \bullet$	Hydroperoxy radical	[-]
$ROO \bullet$	Alkyl peroxy radical	[-]
$ROOH$	Hydroperoxide	[-]
$RO \bullet$	Alkyloxy radical	[-]
$HO \bullet$	Hydroxy radical	[-]
J	Inertia	[kg · m ²]
K	Torsional Stiffness	[Nm/rad]
B	Torsional Damping	[Nm · s]
τ	External torque	[Nm]
$\alpha_1, \ddot{\theta}_1$	Angular acceleration	[rad/s ²]
$\omega_1, \dot{\theta}_1$	Angular velocity	[rad/s]
θ_1	Angular coordinate	[rad]
ω_{nat}	Natural frequency	[rad/s]
C_{crit}	Critical damping	[Nm · s]
P	Power	[W]
Q	Energy	[J]
m	Mass	[kg]

C	Specific heat constant	[J/(kg · °C)]
ΔT	Temperature difference	[°C]
x	Linear coordinate	[m]
\dot{x}	Linear velocity	[m/s]
\ddot{x}	Linear acceleration	[m/s ²]
x_0	Initial coordinate	[m]
v_0	Initial velocity	[m/s]
k	Spring constant	[N/m]
c	Damper constant	[Ns/m]
F	Frictional force	[N]
t	Time	[s]
δx	Small linear displacement	[m]
b	Combined system damping	[Nm · s]
C_i	Curve fit coefficient i	[–]
A_i	Curve fit coefficient i	[–]
T_c	Contact temperature	[°C]
τ_d	Drag torque	[Nm]
CM_{cp}	Combined heat capacity in clutch pack	[J/°C]

Acronyms

AWD	All-Wheel Drive
LS	Limited Slip
PoD	Pin-on-Disc
FM	Friction Modifier
AW	Anti-Wear
DoF	Degree-of-Freedom
ZDDP	Zinc DialkylDithioPhosphate
HRC	Hardness Rockwell type C
PS	Pin Specimen
DS	Disc Specimen
WCTR	Wet Clutch Test Rig
FASTER	Friction Assessment for Shudder Tendency Evaluation Routine

1 Introduction

The demand for All-Wheel Drive (AWD) in passenger vehicles has rapidly increased during the last decade. In Sweden for example, the share of new cars equipped with AWD-systems is rising and approaches a third of the market share [1, 2]. Modern AWD-systems must be seamlessly integrated with vehicles control systems such as anti-lock braking, stability control, anti-spin systems etc., and this sets high demands on accurately controlled torque transfer in varying situations and environments.

Wet clutches are often used in limited slip (LS) applications, such as the center differential in an AWD-system, to provide torque transfer on demand between shafts rotating at different speeds. However, to provide accurate torque transfer by use of a wet clutch, it is essential to be able to predict the friction in the interface between friction discs and separator discs. Therefore, there have been several extensive studies during the last decades to investigate the friction characteristics in wet clutches for LS applications. In these studies, the friction characteristics have been found to be heavily dependent on the lubricant used and the condition it is in [3, 4].

To gain further insight into the mechanisms of oil ageing and its effect on the friction system in wet clutches, further research is required. Current testing procedures are time consuming and often valid for just one specific clutch setup. Therefore this project will focus on developing a method to predict the dynamic response of the wet clutch system to aged oil. This method can be described in three main steps;

1. Simplify friction characterization by Pin-on-Disc model scale testing
2. Develop dynamic model of wet clutch test rig
3. Evaluate clutch system response to degraded oil by using data from point 1 in point 2.

1.1 Background of AWD-systems

The first all-wheel drive system was invented by the Dutch company Spyker in 1903, but it was not until the invention of the Rzeppa constant velocity joint (1927) that all-wheel drive became a practical alternative in drive trains [1]. During the Second World War, the demand for AWD surged when the U.S. military needed vehicles that combined good off-road mobility with reasonable on-road performance. This combination was possible by having a car which was rear-wheel driven (RWD) while on the road, but having a possibility of connecting the front wheels also to the drive train to make the vehicle AWD. This is usually referred to as having “part-time AWD”. A major downside in this setup was that the car had to be stopped while inserting locking pins into the front wheels, and with fully locked differentials the handling on tarmac would instead become problematic.

The reason why combining on and off road performance is difficult, can be seen when studying a car driving through a corner, as seen in Figure 1. All the wheels have individual paths that they travel, meaning they have to turn at different speeds unless something slips. The simplest AWD system will force all wheels to rotate at the same speed, which can be good for traction in off-road conditions, however it will lead to very bad on-road performance.

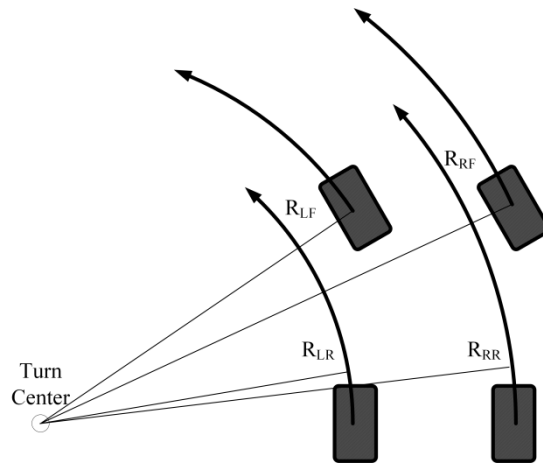


Figure 1. Wheels must rotate at different speeds when turning, due to individual arc length for each wheel when turning.

The real breakthrough in AWD systems for passenger vehicles came during the 1980's when Audi launched the Audi Quattro, since this system enabled good performance both on- and off-track without having to switch between two distinct modes. This was enabled by having a worm-gear type torque biasing center-differential which distributed power to the front and rear axles. A system like this which cannot be deactivated is called "full-time AWD". The main weakness with this system is that in certain conditions, such as one wheel completely losing traction, it will direct all torque to the wheel with no traction in the same manner as an open differential and thereby be unable to drive the vehicle.

During the 1990's, another important system was invented, the Haldex AWD system. This was the first on-demand AWD system and was based on a wet clutch type center differential which was hydraulically activated when a difference in rotational speed between front and rear axles was used to build hydraulic pressure. The great benefit with this system was that it could switch seamlessly from fully open (2WD) to fully closed (AWD) center differential. The downside in the early generations was that the system was reactive, and did not activate until wheel spin already was a fact. By replacing the mechanical hydraulic pumping system with an electric pump, the system could be activated at will by a signal from the vehicles main control unit. This wet clutch based on-demand AWD is the type of system that will be discussed in this work.

1.2 Wet Clutches in AWD

In on-demand AWD, it is essential to be able to precisely control the torque transfer in the center differential. In a wet clutch, torque transfer between input and output shafts is determined by a number of design factors and operational factors. The design factors include the number of friction interfaces (how many clutch plates), and the mean friction radius (radial size of the clutch plates). The operational factors include friction coefficient and axial force compressing the clutch. Since the axial force can be controlled very precisely by hydraulic or electric actuation, the accuracy of the torque transfer will come down to how well the friction coefficient can be predicted.

The schematics of a wet clutch in operation can be seen in Figure 2, where A is defined as the input shaft while B is the output shaft. The friction discs D are attached to the input shaft by internal splines while the separator discs (E) are attached to the clutch drum (C) by external splines. The clutch drum is connected to the output shaft and thereby torque can be transferred from A to B by

compressing the discs. Unlike a dry clutch, the wet clutch operates submerged in oil, with the oil providing cooling and controlled friction levels.

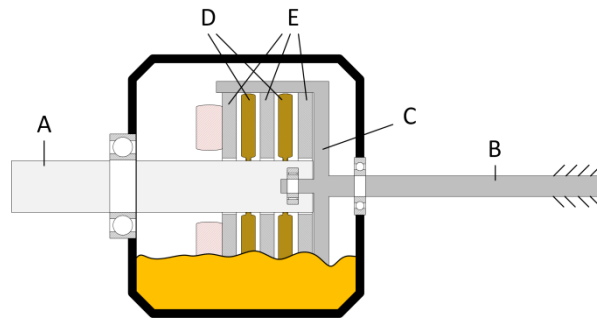


Figure 2. Schematics of important components in a wet clutch.

1.3 Effects of Ageing

The degradation of oil in wet clutches has been shown to significantly affect the friction characteristics [5]. Generally the friction coefficient increases as the oil is oxidized but the increase in friction coefficient is higher at low sliding speeds. If the increased friction coefficient is not correctly compensated for, several problems may occur, for example

- The vehicle dynamics will change which potentially impairs the handling of the car
- The torque transfer will increase which can damage drivetrain components either in the clutch or elsewhere
- Noise, vibrations and harshness (NVH) can reach unacceptable levels

In order to make sure that the AWD-system meets the high quality demands, it is essential to be able to predict the torque transfer over the entire lifetime of the clutch. Ageing models have been developed recently which can be used to compensate the clamping force depending on the state of the lubricant; however, more testing is still required to further improve the predictions, especially for new oil formulations [6].

1.4 Current State

The testing and evaluation of wet clutches can be divided in three main categories; full vehicle testing, component test rigs and model test rigs as seen in Figure 3. In industry, testing is mostly focusing on full vehicle testing and component test rigs. Full vehicle testing is used to completely validate the product but can also be used during development. It is however time consuming which makes it unusable for lifetime testing or oil ageing tests. Currently oil ageing tests often use component test rigs instead where the lubricant is aged while the clutch system operates, the problem with this is that there are normally a limited number of available test rigs and a single ageing test can take weeks. There is however a third category of testing, which can be classified as model tests. These are mainly used in academia and are more generalized than component testing which brings both advantages and disadvantages. The advantages are that model tests are much less time consuming than the other methods, and that they offer much greater control of test parameters.

A disadvantage is that they can be quite far from the real application and therefore requires an interpretation of how the results relate to the real application.

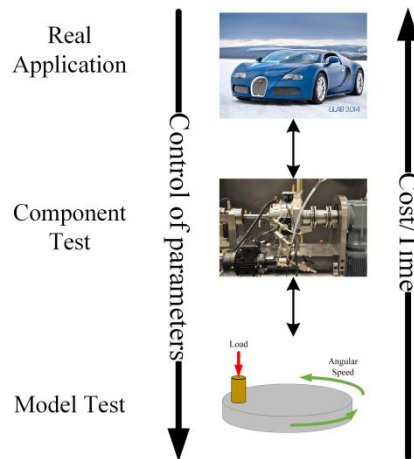


Figure 3. Three broad categories of test methods for wet clutch evaluation.

It has been shown during the last decade that Pin-on-disc model tests can be successfully used to predict friction characteristics in wet clutch systems and should be suitable for screening tests where many oil and material combinations are evaluated [7].

1.5 Objectives

The efficiency of ageing tests could be significantly improved if an artificial ageing method could be combined with a model test to reliably predict the onset of shudder in wet clutch systems.

Therefore, the main objective of this work is to develop a method which combines tribotesting on a model scale with dynamic simulations to predict the performance of oil samples in a component test rig. This method should be fast and reliable and thereby increase the efficiency of lifetime and ageing tests of wet clutch systems. The method should be validated by comparing the predicted system response to experiments in a wet clutch test rig.

2 Wet Clutch Theory

As mentioned previously, the friction in a wet clutch depends on design parameters and operational parameters. More precisely, the torque transfer can be stated as

$$\tau_T = \mu \cdot F_{ax} \cdot R_f \cdot N_{int} , \quad (2.1)$$

where τ_T is the transferred torque, μ is the friction coefficient, F_{ax} is the applied axial force, R_f is the mean friction radius and N_{int} is the number of friction interfaces. Since the latter two of these parameters are fixed by design and the axial force can be controlled, accurate torque transfer relies on determining the friction coefficient during operation. To understand the factors affecting the friction coefficient requires understanding of the tribology of the system; therefore, the following theory contains some of the factors which influence the friction.

2.1 Wet Clutch Operating Conditions

In order to analyze the tribology of the system, it is important to consider the operating conditions of a wet clutch designed for limited slip. Lubricated contacts can be classified into three main lubrication regimes depending on the operating conditions. These are Boundary Lubrication (BL), Mixed Lubrication (ML) and hydrodynamic lubrication (HL). When pressures are high enough to significantly deform the asperities, an additional regime called Elasto-Hydrodynamic Lubrication, (EHL) can be found. The Stribeck curve which was originally determined from journal bearing experiments can be used to distinguish between these regimes. In Figure 4, μ is the friction coefficient and Λ is the film parameter, defined as

$$\Lambda = \frac{h}{\sqrt{R_{qA}^2 + R_{qB}^2}} , \quad (2.2)$$

where h is the actual film thickness and R_q is the root mean square roughness. A rule of thumb is that film parameter values below 1 indicates operation in BL, $1 < \Lambda < 3$ is considered ML, while $\Lambda > 3$ indicates full film lubrication, HL. Since h is very difficult to measure, a combination of sliding speed, ω , oil viscosity, η , and pressure, p , can be used to calculate the Hersey number, H , instead of the film parameter. The Hersey number is defined as

$$H = \frac{\eta\omega}{p} \quad (2.3)$$

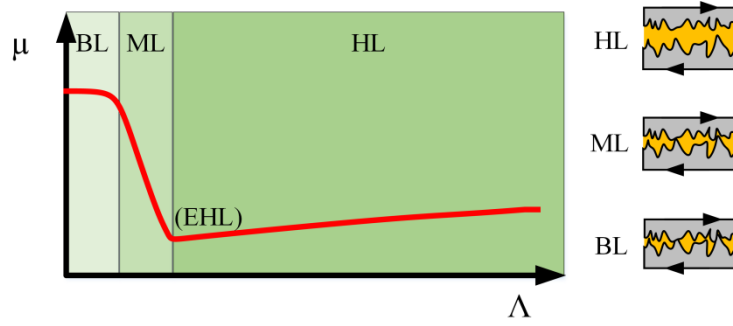


Figure 4. Schematic Stribeck curve showing the relation between surface separation (Λ) and friction coefficient (μ) for lubricated contacts.

The tribological contact in a wet clutch does not have a converging gap and can therefore not build hydrodynamic pressure, which is required to increase surface separation like in a journal bearing operating at high speed. This means that a wet clutch engaged during limited slip will mainly operate in the Boundary Lubrication regime, and therefore the load will be carried by asperity contacts separated only by a thin tribofilm.

2.1.1 Boundary Lubrication and Tribofilm Formation

In the boundary lubrication regime, friction and wear is greatly affected by tribofilms which are formed in the contact. Tribofilms are often formed by specifically tailored oil additives but can also be formed by oxide layers in unlubricated contacts [8]. The tribofilm often consist of a molecule which can be described as having a head and a tail, where the tail is a long hydrocarbon molecule which is soluble in the bulk oil while the head is a polar molecule group that is attracted to the metal surface in the contact. These layers can be in the order of a few nanometers of thickness, which can correspond to a single layer of molecules, called a monolayer. Figure 5 is a schematic description of the micro scale of the contact to the left, and the nano scale with a tribofilm to the right.

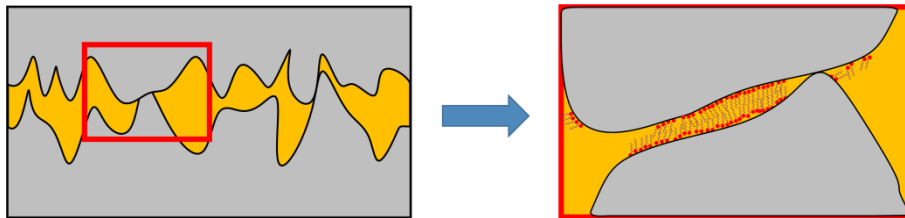


Figure 5. Schematic monomolecular layer adhered to metal surfaces preventing metal to metal contact.

Since the tribofilm will be significantly easier to shear than the metal to metal contact, the overall friction will decrease. Bowden and Tabor called this theory share of metallic contact and described it with the following relation [9],

$$\mu = \alpha_m \mu_m + (1 - \alpha_m) \mu_1 \quad (2.4)$$

where μ_m is the friction coefficient in the metal to metal contact, μ_1 is the friction coefficient in the tribofilm, and α_m is the share of metallic contact, a parameter ranging from zero for a complete tribofilm, to one for pure metal to metal contact, i.e.

$$0 \leq \alpha_m \leq 1 \quad (2.5)$$

2.2 Wet Clutch Components

There are several subsystems that are critical to the function of a wet clutch all-wheel drive system, for example an electronic control unit, a hydraulic system and the actual friction system. In this work, the focus is on the tribological aspects and therefore only the friction system, consisting of clutch discs and a tailored lubricant, will be described.

2.2.1 Clutch Discs

Wet clutches generally have multiple friction interfaces; depending on the required maximum torque transfer capability the number of friction discs may be anywhere from five to ten, with every friction disc having two interfaces. In test rigs however, the number of interfaces may be significantly lower. In Figure 6, a clutch drum and hub is seen to the left and a friction- separator disc pair is seen to the right. The particular material combination shown is well suited to the harsh conditions in a limited slip clutch, i.e. hardened steel separator disc and sintered bronze friction disc.



Figure 6. Clutch drum and hub to the left, friction and separator discs to the right.

Regarding the friction disc, many different materials and groove patterns have been used with varying success[10]. In Figure 7 various friction discs are shown with either bronze or organic type friction liners. Sintered bronze has several advantageous properties compared to organic based friction discs which are common in wet clutches not subjected to extended periods of limited slip. Some of these properties include;

- High heat transfer capability.
- High permeability which improves oil flow and also acts as oil reservoirs during starved conditions [11].
- High stiffness to reduce time taken to compress clutch pack.
- Low cost of production.

The friction disc has a core of hardened steel, which is the same material as is regularly used for the separator disc. Groove pattern is also an important factor, where different manufacturing methods have been shown to affect for example permeability [11].



Figure 7. Different friction liner materials and patterns.

2.2.2 Lubricants

Wet clutch lubricants are composed of two parts; a base oil and an additive package. Lubricants without any additives (pure base oil) have been shown to produce very unfavorable friction characteristics, with higher static than dynamic friction as shown in reference [12, 13] for example. One of the most important aspects of the wet clutch lubricant is to provide predictable friction characteristics, but this is however not the only task to consider when evaluating wet clutch lubricants, some of the other tasks the lubricant must fulfill are;

- Transfer heat out of the contact area
- Protect against wear
- Remove contaminants and debris
- Transfer hydraulic force
- Reduce noise, vibration and harshness

To accomplish this, additives are required. Figure 8 illustrates schematically how the friction characteristics in a wet clutch can change between different oils. This has been shown by several authors, for example [12, 13]. As can be seen, the friction characteristic is heavily altered at low sliding speeds where a fully formulated ATF oil for example usually has a lower static friction coefficient which increases with sliding speed, whereas a base oil has a high static friction coefficient which decreases with sliding speed. Recent research indicates that the high static friction for base oils may be due to capillary forces acting between the clutch plates, which at low speeds increase the axial force compressing the clutch, thereby indicating higher friction at low speeds [14].

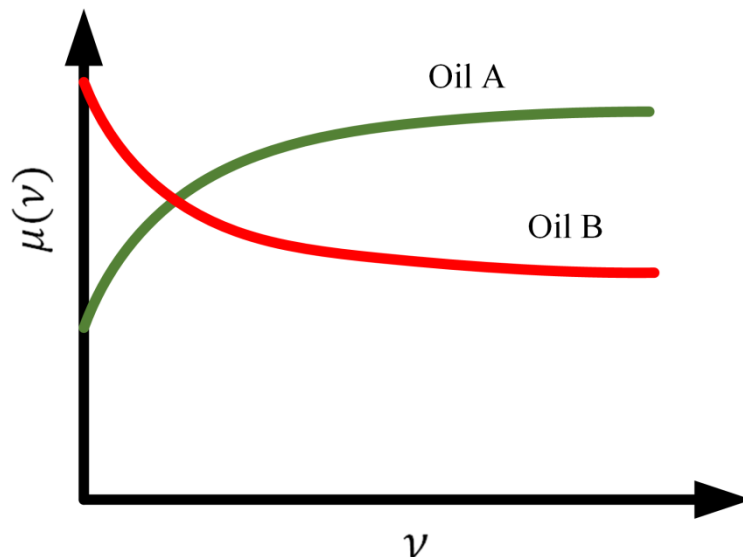


Figure 8. Schematic figure showing difference in friction characteristics for different oils in a wet clutch.

The lubricants used in wet clutches in limited slip applications are subjected to very difficult operating conditions since the lubricant has to withstand severe shearing during the extended periods of slip. For wet clutches used in AWD-systems under limited slip conditions, there are very few available commercial lubricants with proven capability, and therefore the additives used are undisclosed and protected as intellectual property.

2.2.2.1 Additives

Although the exact concentrations of additives can be uncertain, some of the most common additives and their effect on wet clutch tribology will be explained in this section. Additives can be divided into bulk active additives and surface active additives. The surface active additives are most important in wet clutches operating in limited slip conditions since they adhere to the surfaces and have been shown to have a large effect on the friction. Even small concentrations can have a significant effect, as shown schematically in Figure 9, this has been shown thoroughly in reference [13].

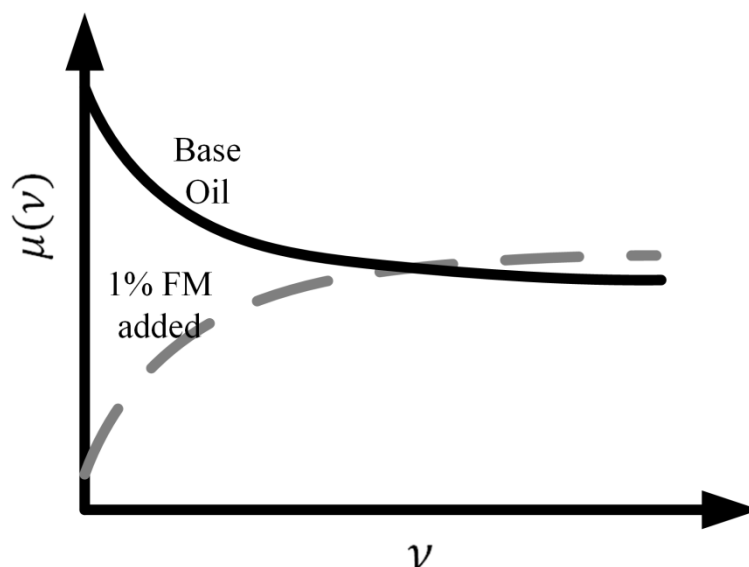


Figure 9. Schematic figure showing the dramatic effect on friction characteristics in a specific base oil for 1% treat rate of friction modifiers.

Common types of additives used in wet clutch applications are friction modifiers (FM), anti-wear agents (AW), dispersants, detergents, anti-oxidants, defoamers, sealing agents and viscosity modifiers [3, 4, 15]. The surface active additives are mainly FM, AW, but also detergents, dispersants or anti-oxidants depending on the exact chemical composition [12, 16]. One of the most common and most important additives used in wet clutch applications is called ZDDP (zinc dialkyldithiophosphate).

ZDDP combines anti-wear properties with anti-oxidant and detergent properties, and since it is surface active it also affects the friction characteristics. ZDDP forms an easily sheared protective layer which is a few tens of nanometers thick. A downside with ZDDP is that it requires a certain temperature to activate, generally at least 60 °C [17].

Fatty acids are other very important friction modifiers. They are hydrocarbon chains with a polar head group which adheres to metal surfaces. Fatty acids can be produced from mineral oils and they are one of the most common friction modifiers [16].

Anti-Oxidants are also very important additives which are added in order to protect the oil from degradation through oxidation. Antioxidants usually contain sacrificial components called radical scavengers which react with free radicals to prevent the free radicals from reacting with other elements in the oil.

2.3 Tribological Failures in Wet Clutches

There are several ways that a wet clutch can fail, but regarding the tribology of the friction system, these failures can be divided into two main categories, as explained in reference [4]. Loss of torque transfer generally means that the friction coefficient is too low so that no torque (or not enough) can be transferred, and therefore the wet clutch has failed. Degraded friction characteristics can be either too high or too low friction at certain operating conditions, but the main problem is that the friction coefficient cannot be predicted with enough accuracy, and therefore the force required to engage the clutch can become either too high or too low. Inaccurate torque transfer leads to undesirable vehicle dynamics, and if the torque transfer is too high, it may also damage driveline components including the clutch itself. Degradation of friction characteristics can also lead to friction-induced vibrations and noise such as stick-slip or shudder, which will be further discussed in the dynamics section.

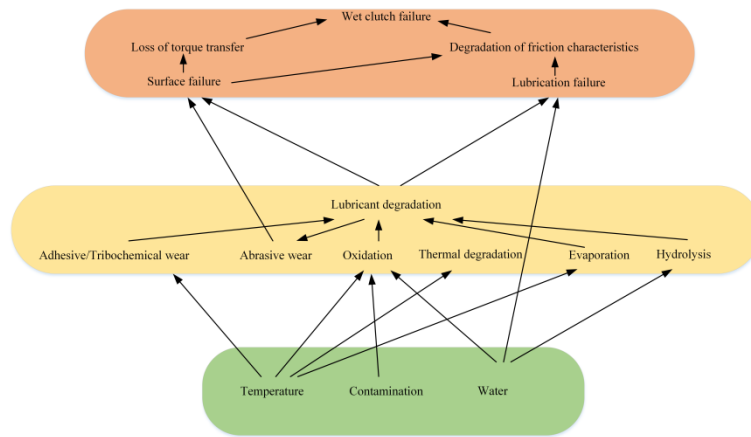


Figure 10. Factors leading to failures of wet clutches reproduced from [4].

2.3.1 Surface Failure

Depending on the materials used in the friction disc, there are various types of failures that can occur. The surface material can be considered to have failed if the friction characteristics change significantly, so that the accuracy of torque transfer is lost. For the sintered bronze materials studied in this work, problems can include excessive amounts of wear particles, which in turn can clog pipes, pumps or the pores of the friction material [19]. Figure 11 shows two different wear mechanisms which lead to delamination wear in copper based friction material; fatigue wear (a) and wear caused by oil-wedge effects (b) [18].

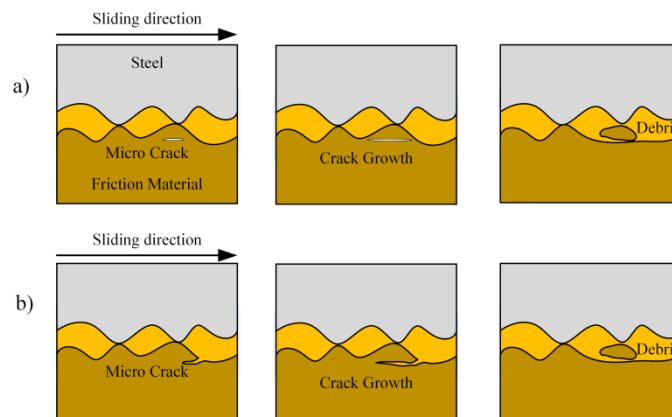


Figure 11. Schematics of delamination wear caused by either fatigue (a) or oil-wedge effect (b) reproduced from [18].

If the oil film is maintained between the clutch discs and the pressure is within the normal operating range ($\sim 1\text{-}10$ MPa), the wear can be considered to be in the mild to ultra-mild wear regime. In this case, micro-plowing and plastic deformation will be the main factors affecting the surface profile [18].

2.3.2 Lubricant Failure

Failure of a wet clutch lubricant usually means that the friction characteristics have become degraded, as described in Figure 10. Factors such as elevated temperature, high pressures or heavy shearing of fluids can generally cause degradation of lubricants in different ways, as described in Figure 12 reproduced from [20].

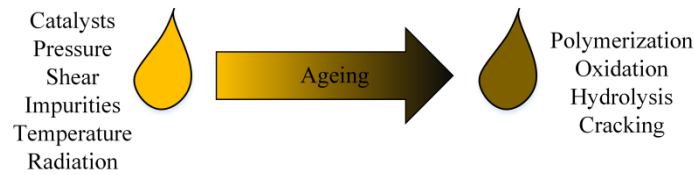


Figure 12. Various factors causing different types of degradation in oil [17].

For wet clutch systems specifically, the most important case of degradation is oxidation, and especially oxidation of additives. The oxidation process is usually described in four steps; initiation, propagation, chain branching and termination of the radical chain reaction [13].

In the initiation stage, a hydrocarbon chain, RH , reacts to form highly reactive but short lived free radicals. The rate of initiation is very slow, however, elevated temperatures (above $60\text{ }^{\circ}\text{C}$) and catalysts such as Cu or Fe increase the rate.



In the propagation stage, the free alkyl radicals react with oxygen to form an alkyl peroxy radical, as shown in reaction (2.7). This reaction is very fast and is insensitive to temperature.



The alkyl peroxy radical formed in reaction (2.7) will in turn react with a hydrocarbon molecule to form a new alkyl radical and also hydroperoxide, according to



The alkyl radical formed can react with oxygen again according to reaction (2.7). Reaction (2.8) has a low reaction rate and will be the limiting factor for the rate of the next step, which is called the chain branching. In chain branching, the hydroperoxide is cleaved into two free radicals:



This reaction requires a high temperature to activate; usually temperatures around $120\text{ }^{\circ}\text{C}$ are required. The products of reaction (2.9) are highly reactive and will further degrade the lubricant, forming ketones and aldehydes.

The final step of the chain reaction is the termination, or autoretardation. In this step, the hydroperoxides are depleted and thereby the chain reaction comes to a halt. This is shown in the schematic diagram in Figure 13, where A is the rate of oxygen uptake and B is the concentration of hydroperoxides [13].

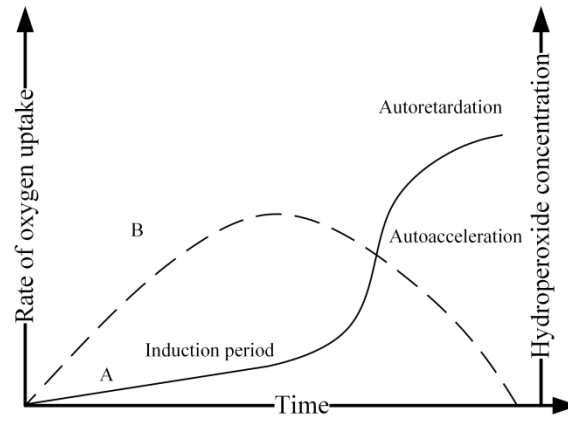


Figure 13. Termination of the oxidation occurs when the hydroperoxide concentration is low. A is the rate of oxygen uptake and B is hydroperoxide concentration. Reproduced from [13].

The effect of oxidation and thereby additive depletion on the friction coefficient in a wet clutch system can be determined with a concept analogous to the share of metallic contact described in section 2.1.1, as shown in reference [6]. Assuming that μ_d is the friction coefficient when using an oil depleted of additives, and μ_f is the friction coefficient when using a fresh fully formulated oil, equation 2.4 can be restated as

$$\mu = \alpha\mu_d + (1 - \alpha)\mu_f \quad (2.10)$$

The parameter α is now related to the condition of the lubricant with regards to oxidation. This parameter has been shown to depend heavily on the temperature and time of exposure to elevated temperature, and thereby the increase in friction with ageing can be predicted for a specific sample, as shown in reference [6] and in Figure 14 below.

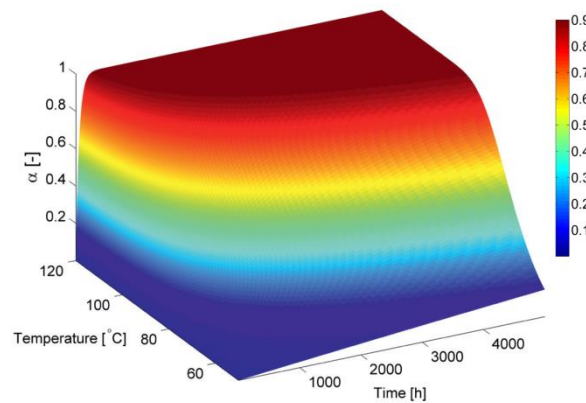


Figure 14. Effect of oil ageing on the parameter alpha, with alpha = 1 corresponding to depleted additives causing increased friction [4].

2.4 Wet Clutch Dynamics

There are several dynamic sub-systems in a wet clutch system; these include for example electronics, hydraulics and mechanics. All systems are important for the accurate function of a wet clutch, however, as this work involves mainly the effect of aged oil on the friction system, only the

mechanics will be considered. The mechanic sub-system includes the thermodynamics as well as the rotational mechanics since these are strongly coupled via the temperature dependent friction behavior.

2.4.1 Rotational Mechanical System

A rotational mechanic system can be described in terms of inertia, J , stiffness, K , damping, B and external torque, τ , at discrete points, this is called a lumped parameter system. A simple rotational system with one degree of freedom (DOF) is shown in Figure 15 below.

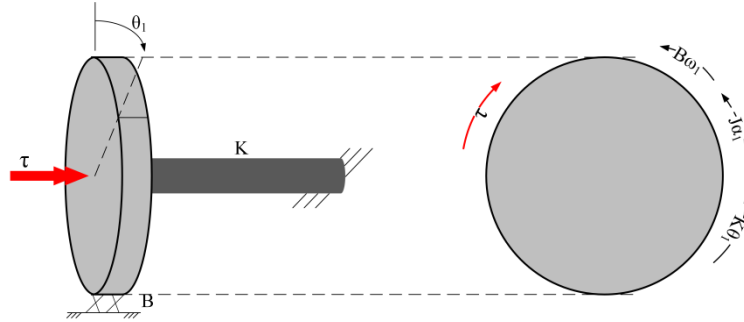


Figure 15. Simple 1-DOF rotational mechanical system, with free body diagram to the right.

According to the free-body diagram in the figure above, the torques acting on this system are the stiffness torque, $K\theta$, the viscous damping torque, $B\omega$, and the applied torque, τ . In addition, the inertial torque, $J\alpha$, is indicated by the dashed arrow. The governing equation is given by conservation of angular momentum,

$$J\alpha_1 + B\omega_1 + K\theta_1 = \tau \quad (2.11)$$

Or expressed in θ only

$$J\ddot{\theta}_1 + B\dot{\theta}_1 + K\theta_1 = \tau \quad (2.12)$$

Selecting θ and ω as state variables leads to a simple system of two linear ordinary differential equations

$$\begin{aligned} \dot{\theta}_1 &= \omega_1 \\ \dot{\omega}_1 &= \frac{1}{J}[-K\theta_1 - B\omega_1 + \tau] \end{aligned} \quad (2.13)$$

Equation (2.13) can be solved analytically if the constants are linear, and otherwise numerical techniques can be applied to find the state of the system.

The undamped natural frequency of the dynamic system is expressed as

$$\omega_{nat} = \sqrt{\frac{K}{J}} \quad (2.14)$$

Finally, the critical damping is defined as

$$C_{crit} = 2J\omega_{nat} \quad (2.15)$$

2.4.2 Thermodynamics

The power generated in a rotating system, P , depends on the torque, τ , and the rotational speed, ω

$$P = \tau \cdot \omega \quad (2.16)$$

If the output shaft is locked from rotation, such as commonly encountered in a test rig setup, then there will be no power output as work and all the power is dissipated as heat instead. The energy, Q , required to increase the temperature by ΔT in a mass, m , of a material with specific heat constant, C , is given by the following relation

$$Q = mC\Delta T \quad (2.17)$$

Taking the derivative with respect to time gives instead a relation for the power to the rate of temperature increase,

$$\dot{Q} = \frac{mC\Delta T}{dt} \quad (2.18)$$

Solving for the temperature increase rate, $\frac{\Delta T}{dt}$, and integrating with respect to time give a relation for the absolute temperature increase, as seen in equation 2.19-20 below.

$$\frac{\Delta T}{dt} = \frac{\dot{Q}}{mC} \quad (2.19)$$

$$\Delta T = \frac{1}{mC} \int \dot{Q} dt \quad (2.20)$$

2.4.3 Stick-slip and Shudder Phenomena

Stick-slip, shudder, or clutch judder are various terms describing self-induced oscillations in clutches. Sometimes these terms are used interchangeably, but normally a distinction is made

between stick-slip and shudder; shudder refers to low amplitude – high frequency oscillations in the clutch interface, while stick-slip refers to lower frequency vibrations where the clutch interface varies between fully locked (stick phase) or sliding (slip phase). A simple stick-slip system is illustrated in Figure 16 by a block pulled over a surface using a spring-damper, as in reference [21].

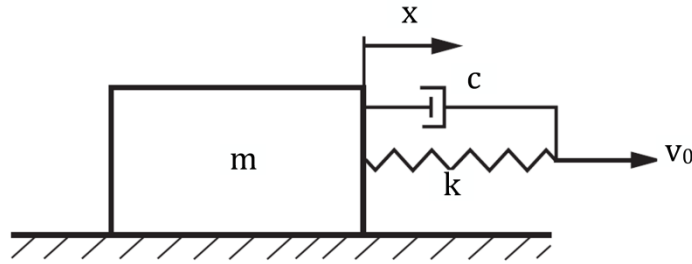


Figure 16. Block pulled over surface by spring and damper.

It can be shown that for a system with zero damping, an instability problem will develop if the frictional force decreases with sliding velocity, and if the frictional force increases with sliding speed the system will slide steadily. Consider the simple frictional pair, seen Figure 16, consisting of a rigid plane and a rigid block of mass m . The block is being dragged with initial velocity v_0 by a spring-damper connection over a rigid surface. The total system stiffness is represented by k , and the damping by c . The resisting frictional force is $F(\dot{x})$. The equation of motion is then

$$m\ddot{x} + F(\dot{x}) + c\dot{x} + kx = kv_0t + cv_0 \quad (2.20)$$

The steady state solution for this differential equation is given by

$$x = x_0 + v_0t \quad (2.21)$$

Where

$$x_0 = -\frac{F(v_0)}{k} \quad (2.22)$$

A stability analysis can be performed by weakly disturbing the system,

$$x = x_0 + v_0t + \delta x \quad (2.23)$$

Substituting equation (2.23) into the equation of motion (2.20) and linearizing with respect to δx gives [Popov]

$$m\delta\ddot{x} + \alpha\delta\dot{x} + k\delta x = 0 \quad (2.24)$$

Where b is the total system damping, described as

$$b = c + \left. \frac{dF(\dot{x})}{d\dot{x}} \right|_{\dot{x}=v_0} \quad (2.25)$$

The following conditions determine the stability of the system:

Stable system:
$$b = c + \left. \frac{dF(\dot{x})}{d\dot{x}} \right|_{\dot{x}=v_0} > 0 \quad (2.26)$$

Unstable system:
$$b = c + \left. \frac{dF(\dot{x})}{d\dot{x}} \right|_{\dot{x}=v_0} < 0 \quad (2.27)$$

For a system with zero damping, i.e. $c = 0$, the stability can be determined directly from the slope of the friction force to sliding speed relation, as shown schematically in Figure 17.

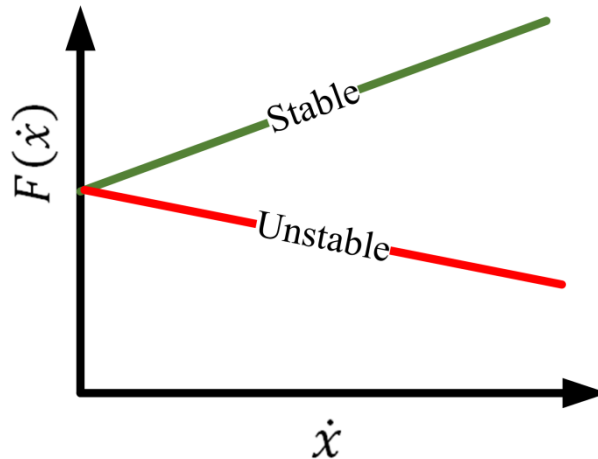


Figure 17. Schematic diagram showing the effect of sliding speed dependent friction force on the stability of a dynamic system.

The frequency of the vibrations is mainly determined by the resonating system and not by the frictional characteristics; however, many tribological factors such as surface roughness and contact conditions will determine the intensity of the acoustic emissions even if they don't affect the frequency spectrum. In wet clutches, shudder or stick-slip leads to unacceptable noise and vibrations, and can in extreme cases also cause permanent damage. It is worth noting that stick-slip and shudder not only causes torsional vibrations, but can also be coupled to activate axial vibrations. A lot of studies have investigated these phenomena, both for clutches and other mechanisms [21, 22]. To reduce the risk of shudder, there are some general guidelines that should be followed [23];

- High damping
- High stiffness
- Positive $d\mu/dv$ -slope
- Roughness $R_a > 0.2 \mu\text{m}$ (prevents adhesive bonding)

Page intentionally left blank

3 Materials and Test Equipment

All experimental equipment used in this work is presented in this section.

3.1 Materials in Friction Interface

The friction interface is composed of a friction material, a counter surface and a lubricant. Several different lubricants are used in this work, while the friction and counter surface materials always represent the specific friction disc and separator disc used in the investigated wet clutch system. These discs can be seen in Figure 18 and the material data is shown in Table 1. The friction material is dispersion sintered bronze lining which covers a disc of hardened steel. The surface roughness of the friction liner is difficult to determine since there are pores with a depth of hundreds of micrometers, but it is significantly rougher than the separator discs.



Figure 18. Friction and separator disc material. Pin on disc test pieces are cut out from the actual clutch discs.

Table 1. Material data for friction liner and counter surface [3].

	Friction Liner	Counter Surface/Core Disc	
Composition	~70wt% Cu, ~20wt% Zn, ~2wt% Sn + Silicon oxide particles Carbon based solid lubricant	Hardened Steel	
Surface roughness Ra	~20	~2	[μm]
Hardness	Brinell ~16	HRC ~40	
Thermal Conductivity	15.7	46	[W/mK]
Specific Heat Capacity	471	449	[J/kgK]

Regarding the lubricants in the interface, there are three distinctly differing oils used in this work. These can be classified as a base type oil, OilB, a model type oil, OilM, and a fully formulated oil, OilF. The specifications for these oils are shown below in table 2. OilF and OilM use the same base but with different additive packages; the former is a fully formulated oil used in the Haldex limited slip couplings produced by BorgWarner, whereas the latter is a model oil which has a vastly reduced additive package. The additive package used in OilF is undisclosed for proprietary reasons,

for OilM however the most important additive is ZDDP. OilB is not intended for use in limited slip couplings, or transmissions at all for that matter. It is a motor oil (15w-40) but is used here to investigate the effects of an oil without the specific friction modifying additives commonly used in wet clutch applications.

Table 2. Lubricant data.

	OilF	OilM	OilB	
Manufacturer	Statoil Lubricants	Statoil Lubricants	Kuwait Petroleum	
Designation	LSC-12-301	SL14-315	Q8 T750	
Base Oil Type	Highly refined mineral oil	Highly refined mineral oil	Paraffinic	
Density at 15°C	866	866	886	[kg/m ³]
Kinematic Viscosity at 40°C	29.0	29.0	104.6	[mm ² /s]
Kinematic Viscosity at 100°C	5.3	5.3	14.0	[mm ² /s]
Thermal Conductivity	0.131	0.131	0.15	[W/mK]
Specific Heat Capacity	2000	2000	2130	[J/kgK]
Relevant additive information	Undisclosed Limited Slip formulation	ZDDP	-	

3.2 Pin-on-Disc Equipment

The schematics of the Phoenix Tribology TE67 pin on disc setup can be seen in Figure 19. The disc sample (DS) is rotating with a specified angular velocity while a load is applied to the pin sample (PS) to generate a pressure in the interface. The sliding speed is calculated from the center of the DS to the center of the PS. Since the PS is very small the difference in true sliding speed from the inner to the outer edge of the PS is negligible. The rotational speed can be held steady between 30 – 1000 rpm with the normal gearing but slower rotational speeds can be measured during start up and slow down. The sliding speed depends on the distance from the PS to the center of the disc but the maximum sliding speed is about 4 m/s. The load cell is a Phoenix Tribology SA800 5Kg and the sampling of all data is at 10 Hz.

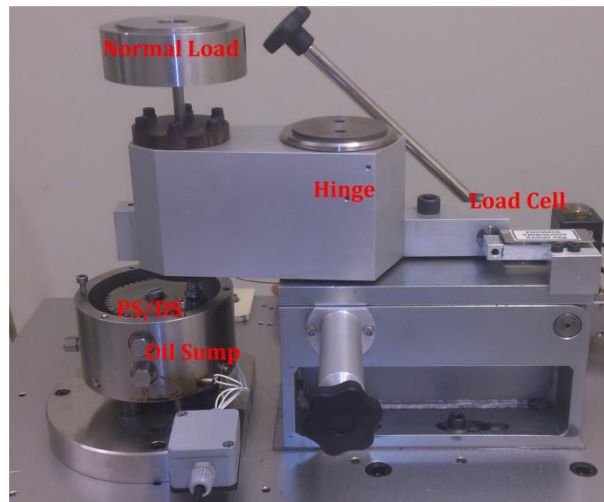


Figure 19. Phoenix Tribology TE67 pin-on-disc test rig.

The lubricant is pumped at a rate of 0 – 250 ml/min from an oil sump below the disc into an oil dispenser located at the center of the disc, see Figure 20. Two 200 W electrical resistance heaters are located in the oil sump and can be used to heat the oil up to maximum temperature of 200°C. Two type K thermocouples are used in this setup; one is mounted at the oil dispenser and one is mounted directly onto the back of the PS. The latter temperature measurement will be referred to as contact temperature, although the thermocouple is mounted 0.1 mm above the interface. Even though the exact interface temperature is not measured this will give an indication.



Figure 20. Oil pumped into oil dispenser located at the center of the disc. Temperature measured in contact and oil outlet.

3.3 Wet Clutch Test Rig

The wet clutch test rig can be seen below in Figure 21. An electric motor (1) powers the input shaft which is connected to the two friction discs located inside the housing (2). There are three separator discs making up the rest of the interface, and these are connected to the output shaft which is mounted to the torque sensor (3). An external oil pump (4) is used to circulate the lubricant from the oil sump into the friction interface. There are forced convection heat sinks mounted to the outside of the clutch housing to provide cooling. The maximum torque supply from the motor is 500 Nm, maximum rotational speed is 317 rpm, maximum contact pressure is 8.6 MPa and the data acquisition rate is at 100 Hz [24].

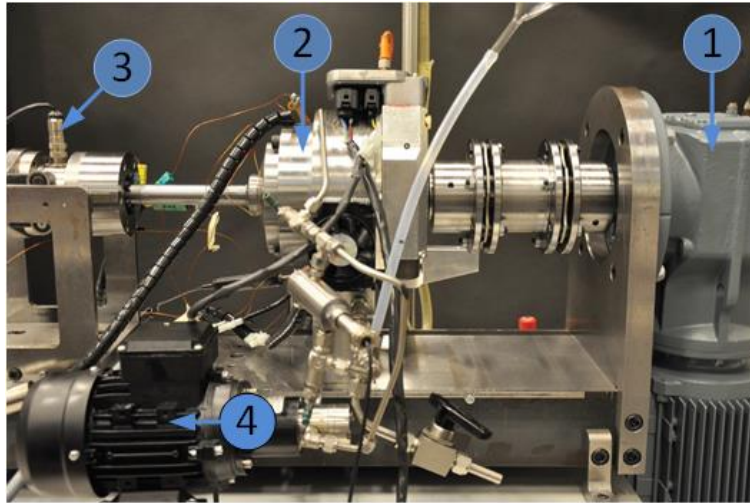


Figure 21. Wet Clutch Test Rig.

Figure 22 shows a schematic view of the wet clutch focusing on the friction system. To the left, the clutch is open and no power flows through the system, while in the right part of the figure the clutch is engaged and torque is applied to the output shaft. Temperature is measured with type K thermocouples located in the middle clutch disc and in the outlet from the clutch drum to the oil sump. Oil is being pumped through the clutch drum into the center of the discs and can be varied from 0 – 1035 ml/min. The entire oil reservoir contains 0.4 liters of oil.

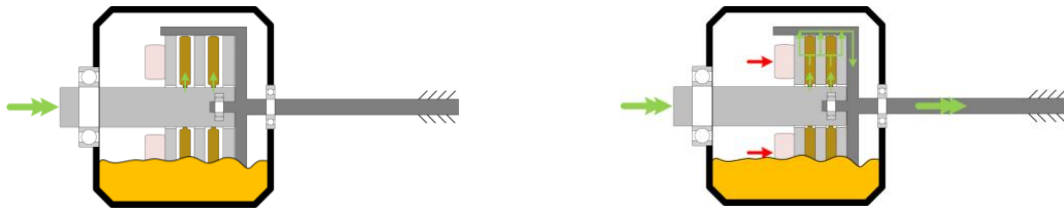


Figure 22. Component test rig schematics; open clutch to the left, closed to the right.

3.4 Auxiliary Equipment

Other equipment and materials used in the experimental procedure are listed below.

- Zygo 7100 3D Optical profiler
- Memert UF75Plus Laboratory oven

4 Part I – Friction Assessment for Shudder Tendency Evaluation Routine (FASTER)

The oil assessment routine is developed in two steps. First, an efficient routine for extracting friction data and generating lookup charts to represent the dependency of friction on sliding speed and temperature is developed. Second, a numeric model using friction lookup charts as input is developed in Simulink to estimate if shudder would occur for a certain oil sample if used in the wet clutch test rig. This routine is described schematically in fig.

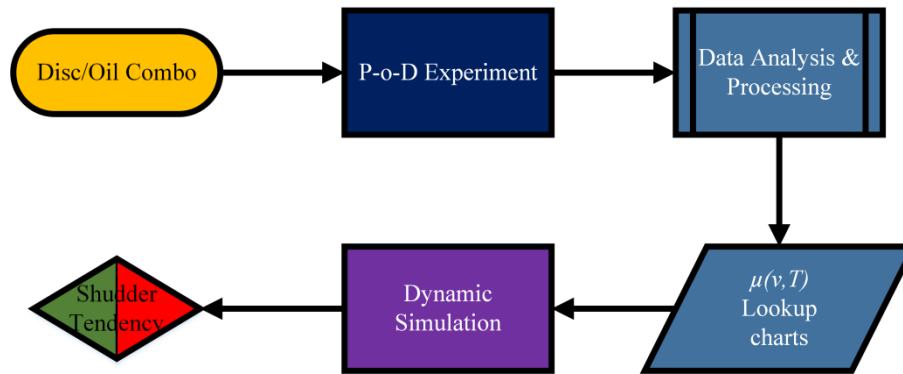


Figure 23. Friction assessment for shudder tendency evaluation routine.

4.1 Friction Assessment by Pin-on-Disc

The friction characterization can also be described in two parts; first, the experimental procedure which generates the friction data is described, secondly, the approach of efficiently handling the data sets and preparing the data for use in the numeric model is described.

4.1.1 PoD Experimental Procedure

For all tests, the contact radius is set to 22 mm. This is the minimum radius that can be used safely without the pin holder contacting the oil dispenser. The reason for choosing a small radius is that the low sliding speeds that are desired in these tests are in the bottom of the range possible with this PoD setup. By choosing a small contact radius, the speed of the PoD can be set higher while producing the same sliding speed. The downside of selecting a small contact radius is that there will be a larger deviation in sliding speed from the edges of the PS as compared to the nominal contact radius. At 22 mm, this difference will be about $\pm 7\%$ which can be compared to the wet clutch test rig with $\pm 15\%$. For oil samples with low levels of additives, PoD experiments tend to have an increased dependence on the individual Pin Specimen (PS) and Disc Specimen (DS) used [5]. To minimize these variations, the effect of the run-in procedure has been studied.

All speed ramps have a duration of 30 seconds.

- i. Heat oil to 30 °C
- ii. Load 0.20 kg
 - a. Increase speed linearly from 0 rpm to 110 rpm (~ 0.25 m/s) during 30 seconds
 - b. Hold for 1 minute
 - c. Decrease speed from 110 rpm to 0 during 30 seconds
- iii. Load 1.2 kg
 - a. Increase speed linearly from 0 rpm to 110 rpm (~ 0.25 m/s) during 30 seconds

- b. Hold for 5 minutes
 - c. Decrease speed from 110 rpm to 0 during 30 seconds
- iv. Load 2.2 kg
 - a. Increase speed linearly from 0 rpm to 110 rpm (~0.25 m/s) during 30 seconds
 - b. Hold for 10 minutes (Short Run-in) or 120 minutes (Full Run-in)
 - c. Decrease speed from 110 rpm to 0 during 30 seconds

To determine the friction characteristics for a certain oil samples, it is necessary to measure the friction coefficient over the entire operating range of temperature and sliding speed. To accomplish this a test procedure is designed where the temperature is increased in levels, while for each temperature level the speed is ramped up and down, before increasing the temperature to the next level and repeating. This is schematically shown in Figure 24 below.

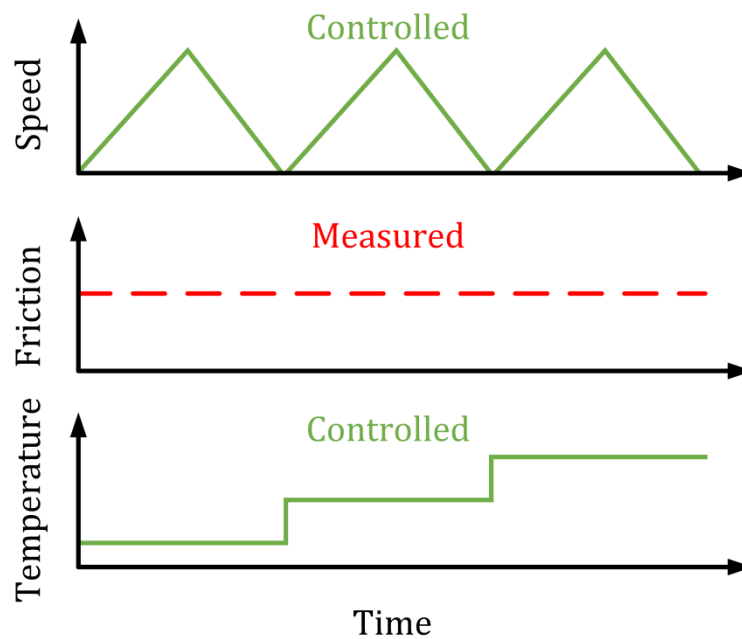


Figure 24. Principle of test procedure to determine friction characteristics over full operational range in pin on disc.

In the actual test procedure the speed will be increased to full speed and decreased back to zero speed three times for each temperature level to improve the credibility of the measurements. All speed increases and decreases have a duration of 20 seconds. The test procedure used is described in steps 1 to 8 below.

- I. Load 2.2 kg
- II. Start oil heater on full power
- III. When oil outlet reaches 25 °C
 - a. Turn down power in heater
 - b. Increase speed to 30 rpm
- IV. Temperature Level 1 reached when contact temperature reaches 30 °C
 - a. Decrease speed to 0 rpm
 - b. Start data logger
 - c. Increase speed linearly to 110 rpm during 20 seconds
 - d. Decrease speed to 0 rpm during 20 seconds

- e. Repeat steps c – d three times
- V. Start oil heater on full power
- VI. When oil outlet reaches 35 °C
 - a. Turn down power in heater
 - b. Ramp speed to 30 rpm
- VII. Temperature Level 2 reached when contact temperature reaches 40 °C
 - a. Decrease speed to 0 rpm
 - b. Start data logger
 - c. Increase speed linearly to 110 rpm during 20 seconds
 - d. Decrease speed to 0 rpm during 20 seconds
 - e. Repeat steps c – d three times
- VIII. Repeat steps V, VI, VII until desired number of Temperature Levels are completed. Standard test setting is 10 °C increments between 40 to 100 °C contact temperature.

4.1.2 PoD Data Analysis

To be able to examine large amounts of oil samples, as well as different pin or disc samples, a generalized routine has been developed for use with the pin on disc equipment. This routine is made up of two Matlab scripts, where the first part is used to import data from the PoD-test and store relevant test settings, while the second part is used to analyze the data and prepare files for use with the dynamic simulation. When importing the experimental data, the experiment settings are stored in three categories; ‘Test Settings’, ‘Hardware Settings’, and ‘Lubricant Settings’ as seen in Figure 25.

From the given inputs, a specific name will be stored for the data. This name gives information about the PS id number and the specific oil sample used. The oil is classified by its bulk content and the level of contamination or degradation. There are three types of oil, OilF, OilM, and OilB, see Table 2 for specifications. Depending on the condition of these oils, they are either marked as A, B or N, standing for Aged, Blended or None. If aged, the time and temperature of the ageing is also stored, while if blended the information regarding type of blender and the volume % at room temperature are stored. The full name will have the format Oil(Y) – (Z), where Y is the bulk oil type and Z is the manipulation of the oil sample.

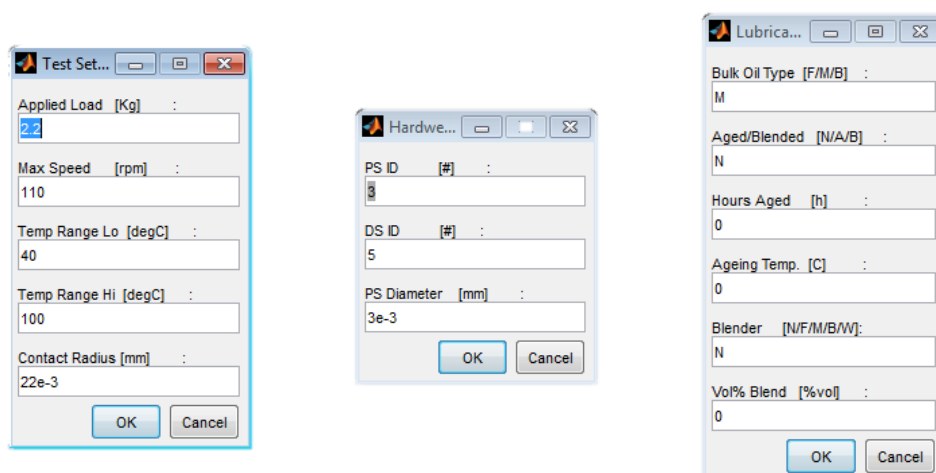


Figure 25. Test-, Hardwear- and Lubricant settings are stored for all tests.

With the information given for contact radius and applied load, the friction coefficient and sliding speed can be calculated. This is presented as seen in Figure 26 below. The left part shows calculated

sliding speed, friction force measured by the loadcell and temperature measured inside the PS. The right part shows the calculated friction coefficient as a function of sliding speed and contact temperature. The seven different temperature levels can be clearly seen in both graphs, and in the left graph the three speed ramps can also be distinguished.

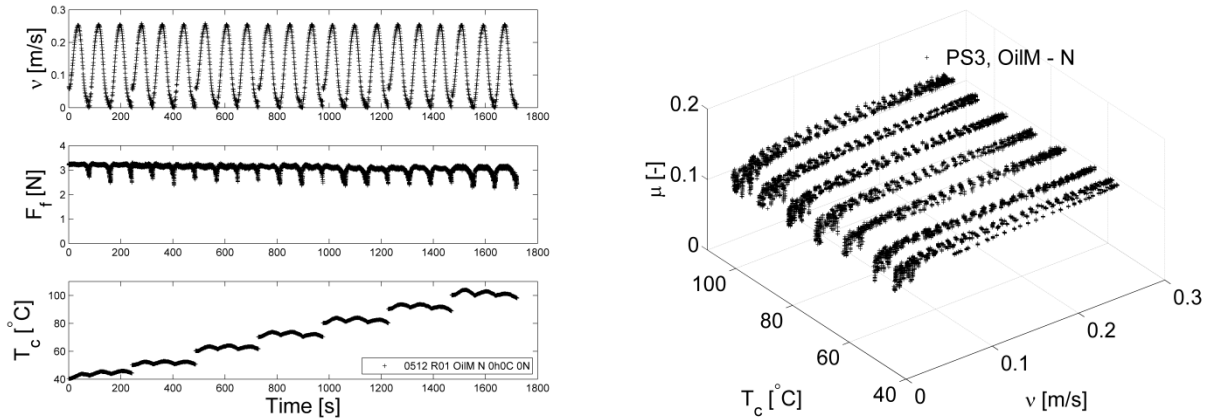


Figure 26. All measured data points for three temperature levels.

The friction data is measured at discrete points in the $T - v$ space, but to be able to use it in a dynamic simulation, a smooth function is required. There are two possible approaches for this; (i) a mathematical function can be found by using curve fitting techniques, or (ii) data can be stored in vectors as a lookup table. Some advantages and disadvantages to both techniques are shown in Table 3.

Table 3. Advantages and disadvantages with using curve fitting or lookup tables.

	Curve Fitting	Lookup Table
Advantage	<ul style="list-style-type: none"> ✓ Smooth well defined function ✓ Used successfully in previous simulations 	<ul style="list-style-type: none"> ✓ Can represent all kinds of friction characteristics ✓ Simple implementation in numeric model
Disadvantage	<ul style="list-style-type: none"> ○ Different oil types may require completely different expression – leads to large number of coefficients in expression ○ Requires a lot of data to produce good fit 	<ul style="list-style-type: none"> ○ Data only at discrete lookup points, must be interpolated in between

Previous curve fit models can be found in reference [25, 4]. A simplified expression is given by

$$\mu = C_1 \tanh(C_2 \cdot v) + C_3 v^{0.1} + C_4 \quad (4.1)$$

While a more general expression that can represent different oil and friction material combinations is given by

$$\begin{aligned} \mu = & A_1 \tanh(A_2 v + A_3) + A_4 \tanh(A_5 v - A_6) - \\ & A_7 \tanh(A_8 v) + A_8 v - \frac{A_9}{A_{10} + A_{11} v} + (A_{12} - T_c)(A_{13} + \\ & A_{14} \tanh(A_{15} v + A_{16}) + \frac{A_{17}}{A_{18} + A_{19} v} + A_{20} v), \end{aligned} \quad (4.2)$$

For large variations in characteristics, the coefficients $C_1 - C_4$ or $A_1 - A_{20}$ must be recalculated for each oil sample. For the same dataset as in Figure 26, the curve fitted function is displayed in Figure 27.

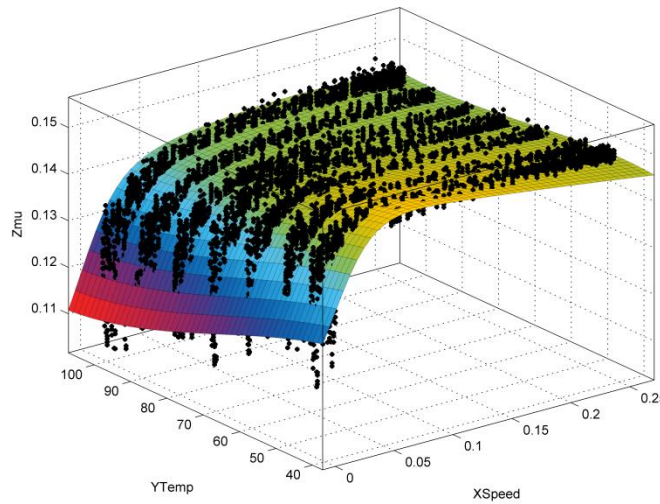


Figure 27. Curve fitted function displayed with data points from PoD test.

In order to use the lookup table approach, some prerequisites must be met. The data points must be arranged in distinct discrete values over the full range, and there must be an interpolation algorithm to find the values in between the discrete points. In Simulink, there are three possible interpolation techniques; flat, linear or cubic spline interpolation. Only cubic spline interpolation gives a smooth function, and therefore the others can be disregarded. However, before the interpolation can be used, the data must be discretized into distinct values, and this can be done by using a so called binning technique. Figure 28 shows the same data as in Figure 26, for the lowest temperature level and with the binning algorithm and cubic spline (CS) interpolation respectively. The red errorbars represent \pm one standard deviation. It can be seen that the cubic spline produces a smooth curve over the data range. Figure 29 shows the final result when plotting lookup bins in three dimensions connected with cubic splines.

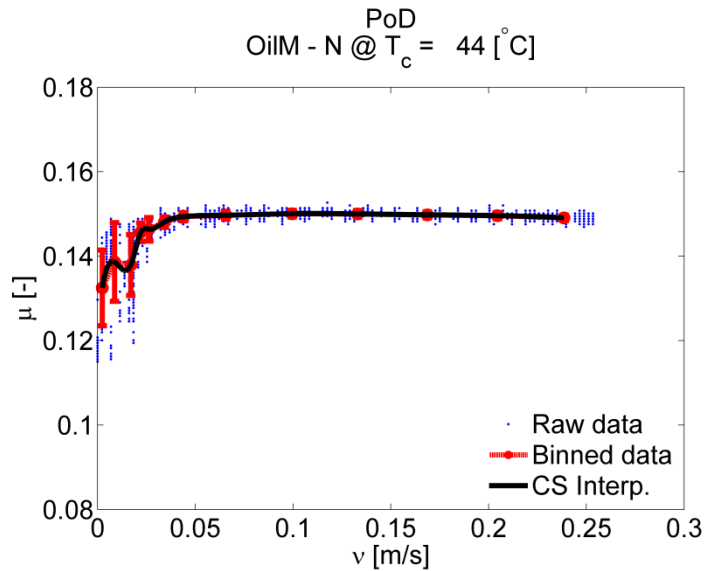


Figure 28. Raw data points grouped in Bins which can be interpolated with Cubic spline function to produce continuous curve.

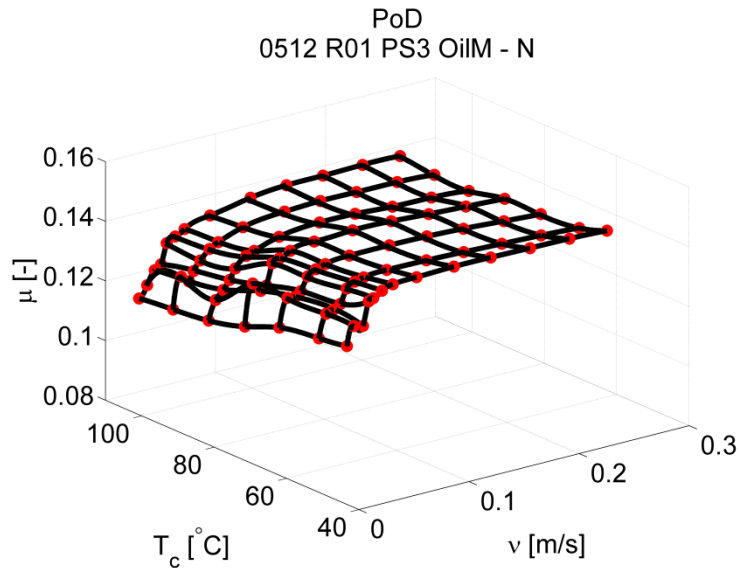


Figure 29. Lookup points in three dimensions, connected with cubic spline function.

From the above evaluation, the binning with cubic splines is selected as the method to use. The great simplicity of representing all kinds of friction characteristics and ability to use relatively crude data sets is a big advantage since this model should be useful when quickly evaluating large amounts of oil samples. Another advantage is that no prior assumption of the $\mu - v - T$ relation is required, and therefore this way arbitrarily shaped $\mu - v$ curves such as the ones described in reference [26] can easily be represented. The binned data points are saved as “.mat-files” containing all information required to construct a lookup table.

4.2 Dynamic Simulation of Wet Clutch Test Rig

The dynamic model consists of three important subsystems; a dynamic motion subsystem, a thermodynamic subsystem, and the friction lookup function. The relations between these are shown schematically in Figure 30 below.

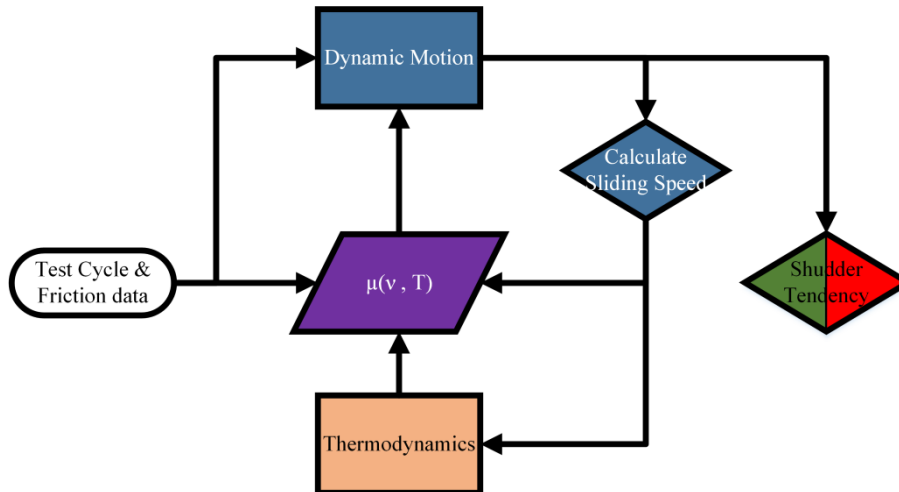


Figure 30. Dynamic simulation consisting of three major subsystems; motion, thermal and friction functions.

A 3D-model of the WCTR with the central housing removed can be seen in Figure 31 below. To the far left is the torque the torque sensor, the electric motor is located to the right and the actual wet clutch with its friction system is in the middle. The hydraulic system is not shown in this view. To create a dynamic model of this system, some simplifications will be made.

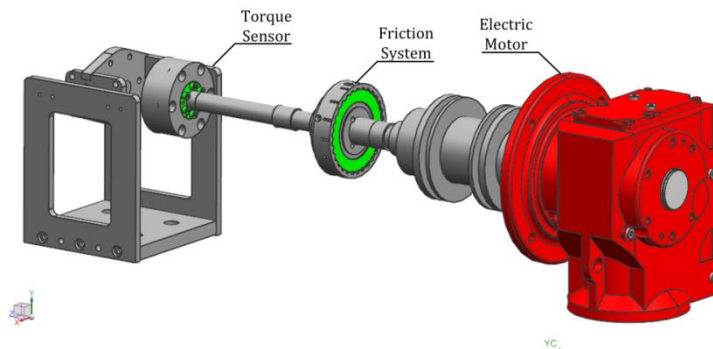


Figure 31. CAD model of WCTR.

As can be seen in Figure 31, the input shaft is of a significantly larger dimension than the output shaft. Therefore, it is a reasonable assumption that the input shaft can be considered rigid. The electric motor has a torque capacity of over 500 Nm and can therefore be considered as having an infinite torque in relation to the torque transferred in the clutch. This means that the system can be modeled by torque acting directly on the separator discs connected to the clutch drum. Figure 32 displays the output shaft with a single separator disc which represents the simplified system.

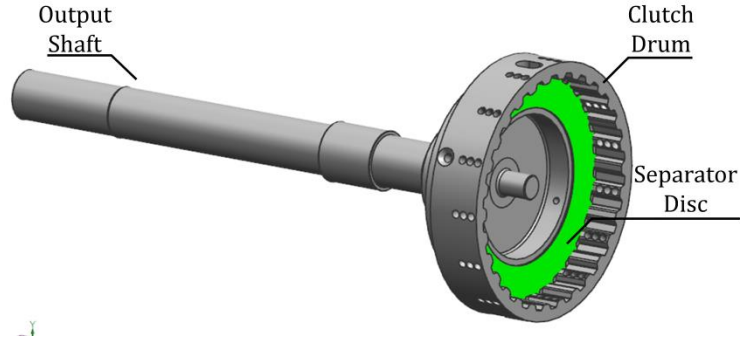


Figure 32. Output shaft with a single separator disc in clutch drum.

For this simplified system, the equation of motion can be used with one degree of freedom exactly as derived in the theory section, stated again in equation 4.3 for convenience. In this case however, τ is the sum of all external torques acting on the system. The Stiffness and Inertia coefficient are easily calculated since the dimensions are well known, the damping however is more difficult to determine, literature studies range from lightly damped at around 1% to heavily damped at ~10% internal damping for a 1-dof model [27].

$$\dot{\omega}_1 = \frac{1}{J} [-K\theta_1 - B\omega_1 + \tau] \quad (4.3)$$

The damping can also partly be modeled as an external torque, in wet clutches the external torque, τ_d , generated by viscous damping can be estimated from the shearing of the lubricant in between the clutch plates and follows the relation

$$\tau_d = R_f \cdot N_{int} \cdot A_{int} \cdot \eta \cdot \frac{v}{h} \quad (4.4)$$

Where A_{int} is the interface contact area, η is the dynamic viscosity and h is the film thickness. This relation is only valid when the clutch is disengaged so that full film lubrication conditions occur. In the boundary lubrication regime with a film thickness in the order of a few micrometers, this relation does not hold. In this work however, there is no need for modelling the system when the clutch is disengaged and therefore the damping will instead be described as a general viscous damping according to the following equation

$$\tau_d = B_d \cdot \dot{\theta}_1 \quad (4.5)$$

An alternative description could be to use equation (4.4) with only the area of the grooves in the clutch discs, but due to the uncertainties in the film thickness in combination with the heavy dependency on it, it may be better to adjust the damping empirically.

Another resisting torque is attributed to bearings and seals in the clutch. This is often modeled as a constant torque acting in the direction opposite to the rotation of the output shaft, however, in this model it will be considered included in the general viscous damping of equation (4.5) above

because of the uncertainties of bearing damping at the very small angular vibrations of the locked output shaft.

The dynamic model for the 1-dof system described above is shown in Figure 33. The unmarked input in the bottom left is the external torque generated in the friction interface. The output marked $th1d$ ($\dot{\theta}_1$) is the angular speed and is used to calculate the sliding speed in the interface.

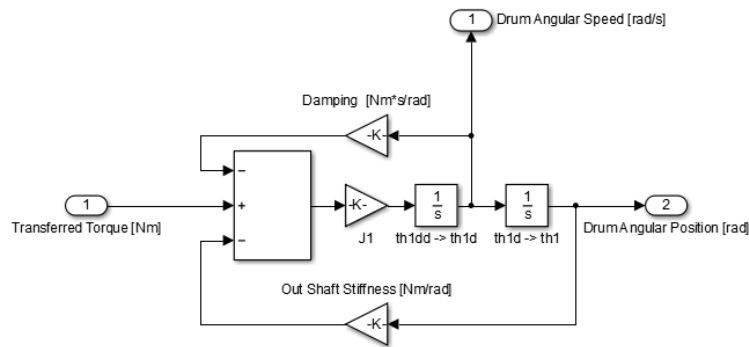


Figure 33. 1-DOF dynamic motion sub-system of WCTR.

Another important sub-system is the thermodynamics of the wet clutch. This system is based on the relations derived in the theory section and models the heat generation in the clutch pack with subsequent heat transfer from the clutch pack to the oil and further to the wet clutch housing, as seen schematically in Figure 34. The housing has a significantly higher heat capacity than the rest of the system, and there are also fan-cooled heat sinks mounted to the housing. Therefore, the housing will be modeled as a constant temperature heat sink as shown in Figure 35.

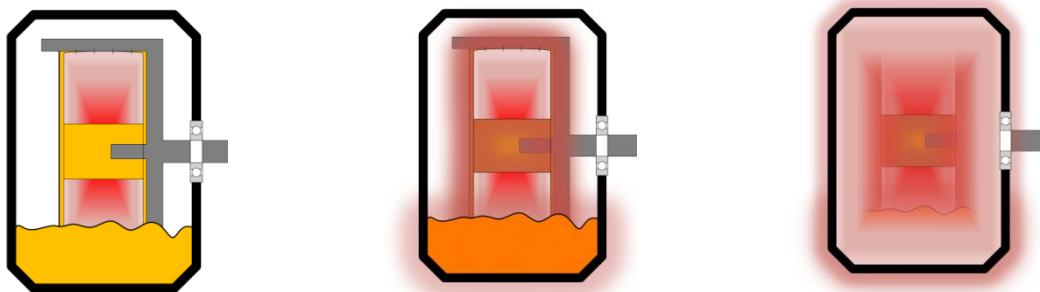


Figure 34. Illustration of the three layers in the thermodynamic sub-system, from left to right; heat generated in clutchpack is transferred to the oil, and finally to the constant temperature housing.

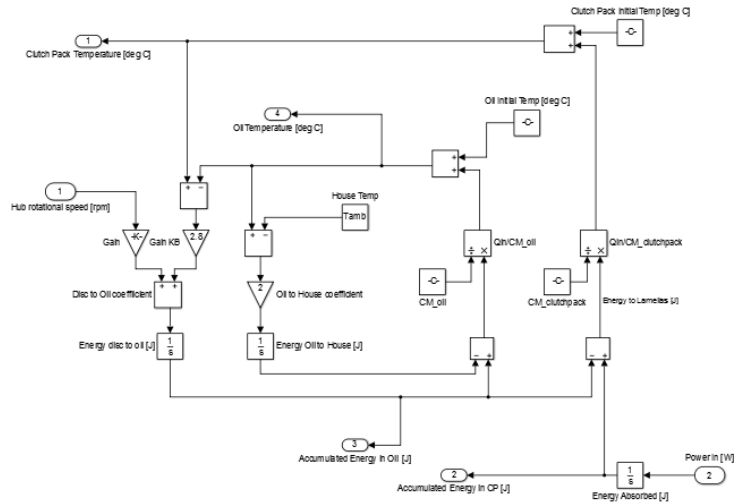


Figure 35. Thermodynamic sub-system with three layers; clutch pack, oil supply, and housing.

A summary of important parameters used in the dynamic simulation are shown in Table 4 below. The numeric solver used is ODE45 Dormand – Prince, with variable step sizing and a minimum step size of 5e-4 s.

Table 4. Constant parameters used in dynamic simulation.

Property	Symbol	Value	Unit
Inertia	J	0.0048	[kg · m ²]
Stiffness	K	9.6653e+03	[Nm/rad]
Damping ratio	C_{ratio}	0.10	[–]
Natural frequency	ω_{nat}	1.4253e+03	[rad/s]
Critical damping	C_{crit}	13.5629	[Nm · s]
Friction radius	R_f	0.0457	[m]
Number of interfaces	N_{int}	4	[–]
House Temperature	T_{amb}	25	[°C]
Combined Heat Capacity of Clutch Pack	CM_{cp}	742.9	[J/°C]

5 Part II – Demonstration of FASTER

In this section, the method developed in Part I will be first validated, and then used to assess the oil condition and estimate if shudder would occur in the wet clutch test rig for various degraded oil samples.

5.1 Validation of FASTER

Validation is performed by combining test results from three types of oil samples; (i) full formulated oil, OilF, which is known to give smooth friction characteristics and thereby avoid shudder at normal operating conditions, (ii) base engine oil, OilB, which is known to cause shudder due to its ill-suited friction characteristics caused by lack of friction modifying additives, and finally, (iii) a blended oil, OilB-B:X%F, which is mainly the same base oil as OilB but blended with X% full formulated oil until shudder ceases to occur in the wet clutch test rig. The idea is to find the limit for when shudder occurs and use it to validate the method of using processed data from the PoD experiment in the dynamic model.

5.1.1 Establishing Shudder Limit in Wet Clutch Test Rig

In order to be able to verify the model, the first step is to find the shudder limit. Therefore, this test starts with OilB which is assumed to cause shudder and then gradually injects fully formulated oil, OilF, which is assumed to prevent shudder into the system. The overall test procedure is summarized in the following four points;

- I. WCTR is filled with 0.4 L of OilB
- II. Run Test cycle x10 or until occurrence of three consecutive audible shudders
- III. Inject 10 ml OilF
- IV. Repeat previous two steps until shudder no longer occurs.

The reason for not allowing more than three consecutive audible shudder tests is to minimize the risk of damaging the test rig or its sensors from the violent vibrations. The injection of OilF into the system can be seen in Figure 36. After injecting the oil the clutch is rotated at 100 rpm for 2 minutes to mix the oil before proceeding with the next shudder test again. The oil flow is set to the maximum of 1035 ml/min during both mixing and the actual test cycle.

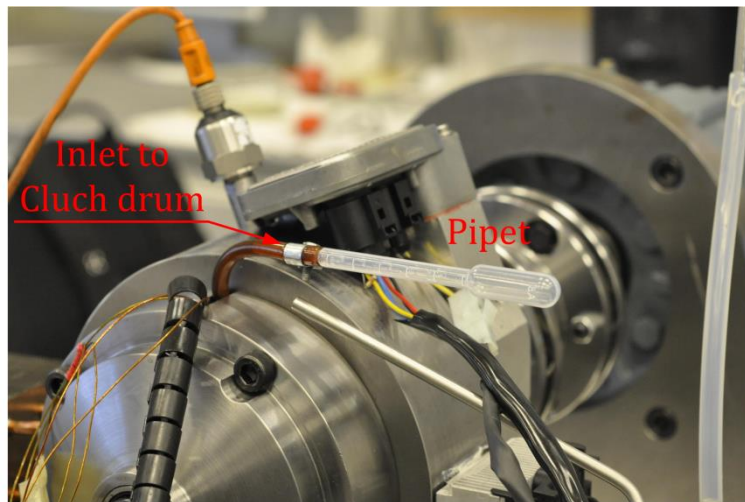


Figure 36. Injection of fully formulated oil into the clutch drum inlet.

The test cycle proceeds in the following steps which are also shown in Figure 37.

1. 4 kN Load is applied
2. Speed is increased to 1 rpm and held constant for 5 seconds
3. Speed is increased linearly to 50 rpm during 30 seconds
4. Speed held at 50 rpm for 1 second
5. Speed decreased linearly to 0 rpm during 3 seconds
6. Wait for temperature in clutch disc cool down to 40 °C then repeat from 1.

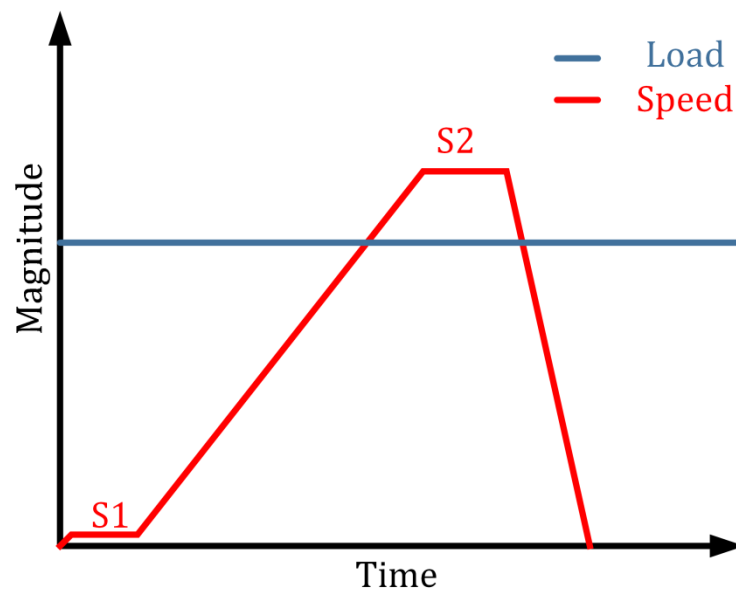


Figure 37. Test procedure for shudder limit in wet clutch test rig.

When the shudder limit has been determined, the oil sample is extracted from the WCTR and stored for analysis with the FASTER method previously described.

5.1.2 Analysis of Shudder Limit Oil by FASTER

After the shudder limit has been determined, three oil samples will be analyzed with the previously described FASTER method. These are OilF, the fully formulated non-shuddering oil, OilB, the full-shuddering base oil, and OilB-B:X%F, which is the shudder limit oil which is on the verge of causing shudder. These oil samples are evaluated in accordance to the procedure described in section 6.1.1, with temperatures ranging between 30 to 100°C.

The next step is to process the data according to the routine described in 6.1.2 and produce the charts which relates the friction coefficient to sliding speed and temperature. This data processing only takes a couple of minutes with the prepared routine before the dynamic model can be used to estimate if shudder would occur in the test rig. Initially, only 10% linear viscous damping is used before.

5.2 Evaluation of Degraded Oil by FASTER

In this section, oil samples are degraded by both thermal ageing and water contamination, and then assessed with the method described in sections 6.1-2. The degradation methods are not intended to fully replicate the complex process of ageing and degradation which occurs in operational wet clutches in all-wheel drive systems; however, if the performance of the oil mainly relies on the $\mu - \nu$ relationship then the manner of how the degradation occurred may be of less importance for demonstrating the capability of this method.

5.2.1 Thermal Ageing of Oil Samples

For the thermal ageing, OilM is selected since it is a model oil containing no anti-oxidants except for ZDDP and is therefore likely to react faster than for example the fully formulated oil, OilF. Seven oil samples of 100 ml each are inserted into the laboratory oven at 120°C, as seen in Figure 38. Oil samples are then extracted after 24h, 48h, 96h, 120h, 168h, 288h, and 344h. One sample of OilF was also aged and extracted after 168h. When extracted the oils are evaluated with the routine described in section 6.1-2.



Figure 38. Thermal ageing in Memert Laboratory oven at 120°C.

5.2.2 Oil Degradation by Water Contamination

The water contaminant test was initially intended to be used for finding the shudder limit, therefore the procedure follows the steps outlined in section 5.1.1. In this case however the bulk oil used was OilM, and distilled water was injected at 2 ml per contamination step into the clutch drum of the wet clutch test rig. The test was stopped at 6% vol (7% weight) after torque fluctuations occurred and the oil was analyzed with the routine described in section 4.1-2.

6 Results & Discussion

The results will be presented in three main parts; first, the validity of the overall method will be examined by comparing the results from the wet clutch test rig to the results predicted with the Friction Assessment for Shudder Tendency Evaluation Routine (FASTER). Secondly, factors which could influence the accuracy of the prediction are discussed, such as run-in of PS and bin distribution in the sampling will be discussed. Finally, findings from aged and degraded oils will be presented.

The results disposition is summarized below:

1. Results Validating FASTER
 - a. Prediction of FASTER
 - b. Established Shudder Limit in WCTR
2. Factors Influencing Accuracy of FASTER
 - a. Effect of Aligning and Condition of Pin Specimen (PS)
 - b. Effect of Bin Distribution
3. FASTER Prediction for Aged and Degraded Oils

The naming convention is stated again below for convenience. Three types of bulk oil are used, OilF, OilM, and OilB. The specifications for these oils can be found in Table 2. Depending on the condition of these oils, they are either marked as A, B or N, standing for Aged, Blended or None, so that the pure model oil will be called OilM – N, for example. If the oil has been blended it will be reflected by the volume % and type of blender, either W for distilled water, or F for fully formulated oil. An example of such a name would be OilB – B: 5%F, which is OilB blended with 5% of the fully formulated oil.

6.1 Results Validating FASTER

To validate the method, the same oil samples used in the WCTR will be evaluated with the PoD processing and analysis routine to predict if shudder would occur in the WCTR. This will be compared to actual measurements from the WCTR. All temperatures from the WCTR describe the contact temperature as registered by the thermocouple mounted on the middle separator disc.

6.1.1 Prediction of FASTER

Results from the pin-on-disc test with four different oil samples are shown in this section. All these tests use the same pin and disc specimen and running in was performed according to the procedure described in section 4.1.1. The applied load was 2.2 kg which corresponds to a nominal pressure of 3.2 MPa and the temperature was increased in steps of 10 °C according to the procedure described in 4.1.1. In the figures below, a total of 13 bins were used with the bins packed more densely at low sliding speeds. Note that the measured temperature may be slightly higher than the nominal temperature levels due to the heat generated by friction. The test is however always initiated when the contact temperature corresponds to the nominal temperature level. In Figure 39 and Figure 40 below, the temperature dependency of the four oil samples are shown.

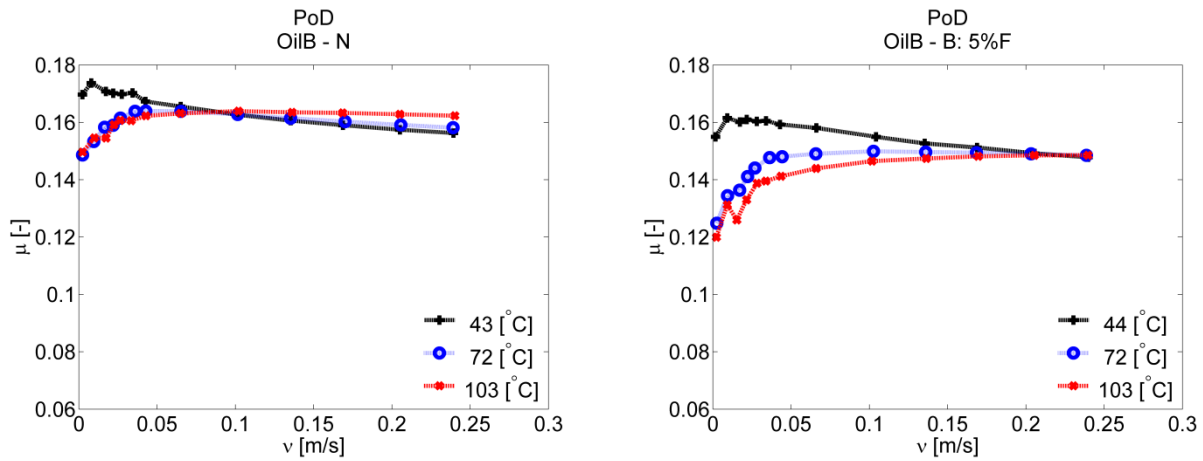


Figure 39. Friction versus sliding speed at three different temperature levels for pure OilB to the left and OilB blended with 5 % fully formulated oil (OilF) to the right.

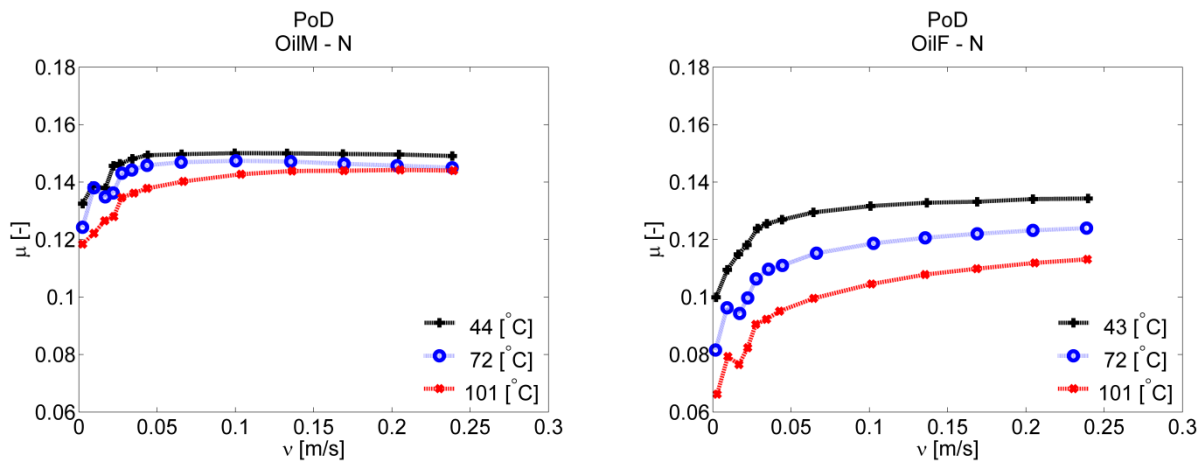


Figure 40. Friction versus sliding speed at three different temperature levels for pure model oil to the left and fully formulated oil to the right.

As can be seen above, Oil B and OilB – B:5%F clearly gives a negative friction to sliding speed relation at the 40°C temperature level, but improves at higher temperatures. OilM and Oil F on the other hand are neutral or positive for all temperatures shown. The fully formulated oil has the lowest friction coefficient and also the most positive relation for $\frac{d\mu}{dv}$. Slight fluctuations at low sliding speeds can be seen in all figures; this may be a property of the testing method instead of the oil and material combination and could be avoided by reducing the bin resolution, this will be further discussed in section 6.2.2.

In Figure 41, the same four samples are compared at the 40 and 100 °C temperature levels. In this comparison, the difference in magnitude of the friction coefficient becomes more clear. The friction coefficient of OilB is around twice the magnitude of the friction coefficient for OilF at low sliding speeds. The difference between OilB and OilB – B: 5%F is quite small at low temperatures, but increases at higher temperatures. This is likely due to the presence of friction modifying additives which becomes activated at higher temperatures, such as ZDDP.

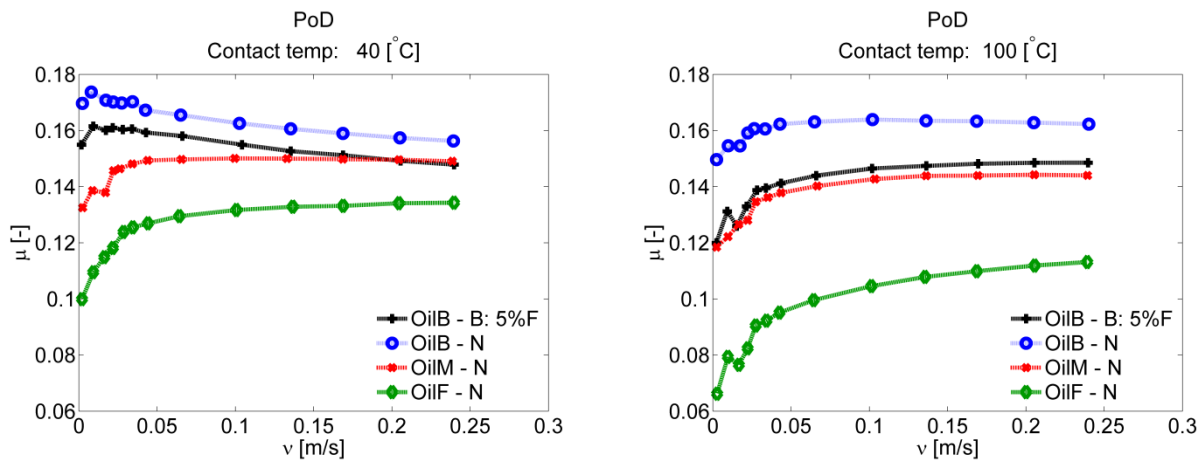


Figure 41. Friction versus sliding speed at a nominal contact temperature of 40 °C to the left, and 100 °C to the right, for the four different oil samples investigated in this range.

Figure 42 shows the results from an additional pin-on-disc experiment which was performed at a temperature range from 30 to 50 °C, since the WCTR only produced shudder at these contact temperatures. Here the water contaminated oil, OilM – B: 6%W is also shown, and it is clear that the water contamination does not degrade the friction characteristics in a way likely to produce shudder in the investigated friction system. The water contaminated oil is actually more similar to the fully formulated oil, with a positive friction to sliding speed relation over the entire measured sliding speed range. OilB blended with 5% fully formulated oil can be seen to slightly improve from 30 to 50 °C, and the same is true for pure OilB, but the changes are very small.

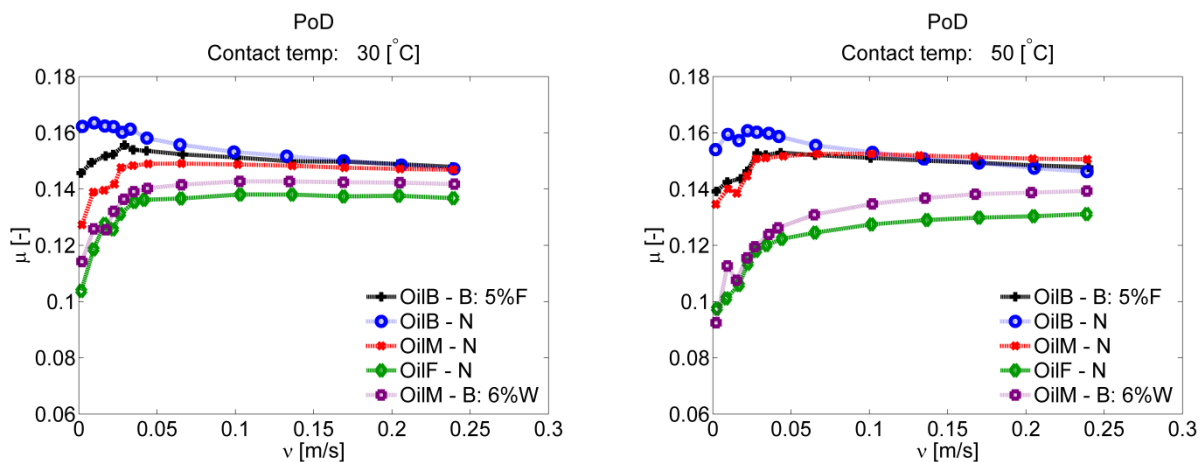


Figure 42. Friction versus sliding speed at a nominal contact temperature of 30 °C to the left, and 50 °C to the right, for the five different oil samples investigated in this range.

In Figure 43 and Figure 44, the full friction maps as functions of sliding speed and contact temperature are shown for OilB, OilF, and OilM. Note that by using the binning and cubic spline interpolation technique very sparse data sets can be used, as seen in Figure 44. Unlike when using curve fitting techniques, a shorter data set will not significantly affect the accuracy of the friction map when using this interpolation approach.

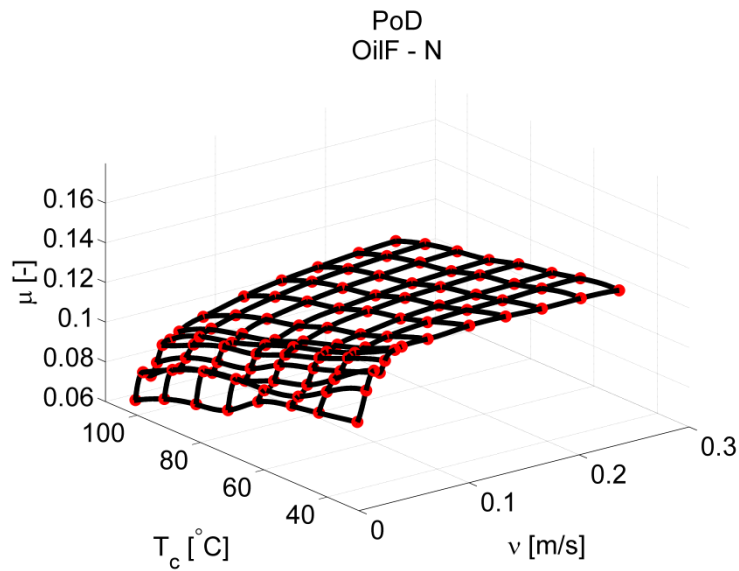


Figure 43. Friction versus sliding speed on the-x axis and contact temperature on the y-axis for fully formulated oil as measured in the pin-on-disc, with cubic spline interpolation between binned data points.

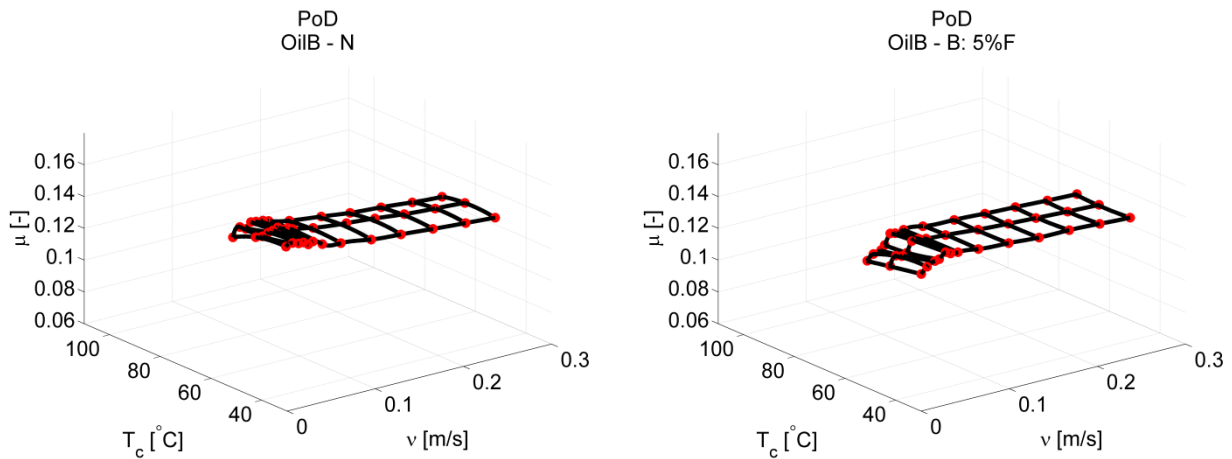


Figure 44. Friction versus sliding speed on the-x axis and contact temperature on the y-axis for fully OilB to the left and OilB blended with 5% OilF to the right, as measured in the pin-on-disc, with cubic spline interpolation between binned data points.

The test cycle used in the dynamic simulation is shown in Figure 45. The axial load and motor speed follows nominal values used in the WCTR experiment. Since there is no coupling between axial load and torsional vibrations any shudder will not affect the applied load, unlike in the WCTR.

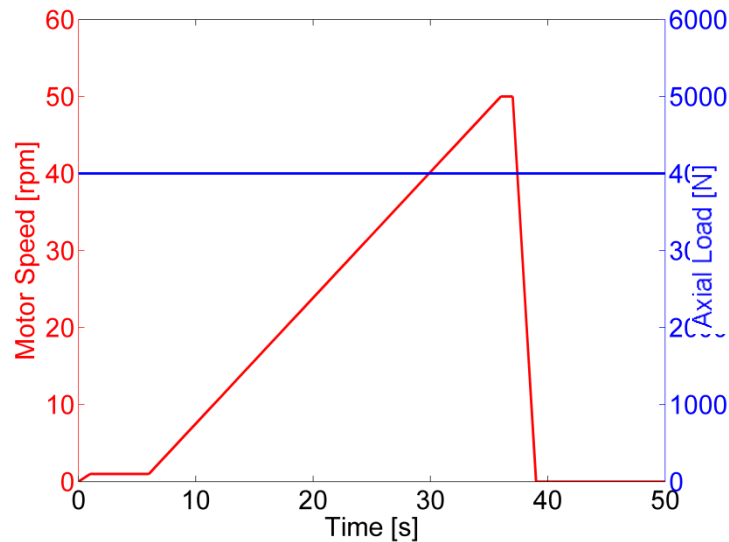


Figure 45. Controlled motor speed and applied axial load used in dynamic simulation.

The predicted torque from the dynamic simulation, using 10% system damping, is shown in Figure 46 and Figure 47 below. As can be seen, severe shudder is predicted for OilB – N, whereas the shudder is milder for OilB blended with 5% fully formulated oil. For the model oil, no shudder is predicted regardless of water contamination. These results correspond reasonably well to the experimental findings, the shudder is most severe for pure OilB and is at the limit of shudder when blending with 5% OilF, whereas no shudder was detected when using OilM. The amplitude of fluctuations are similar at the limit of shudder, but the overall torque levels are higher by about 10% for the simulation, which is caused by a higher friction coefficient being measured in the pin-on-disc.

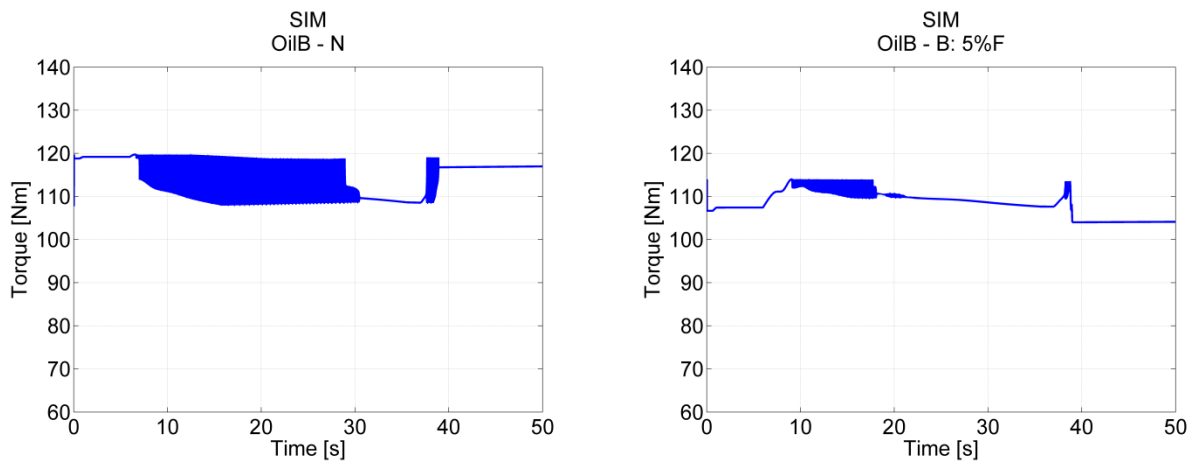


Figure 46. Torque predicted with dynamic simulation exhibiting severe shudder for OilB – N, and milder shudder for OilB blended with 5% OilF, both simulations at 30 °C initial contact temperature.

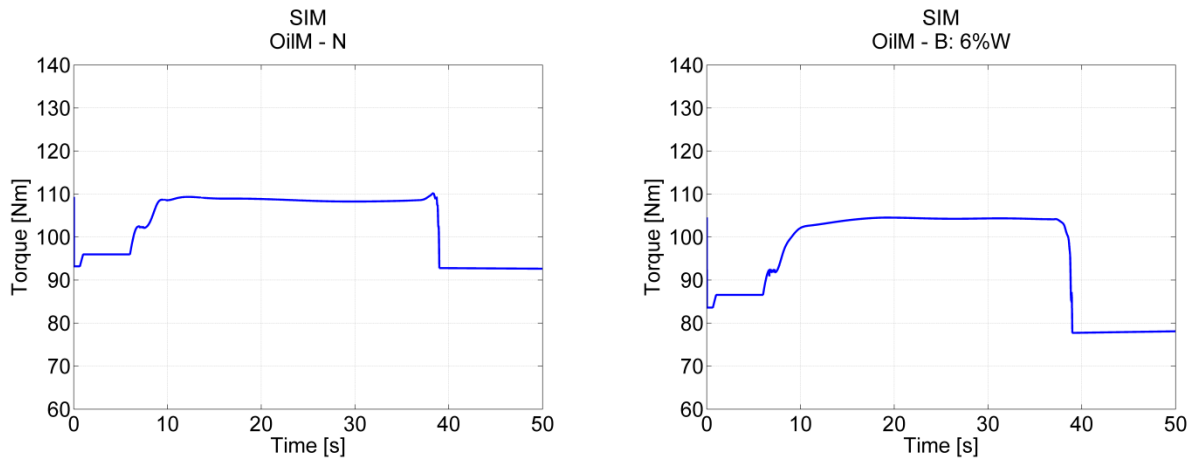


Figure 47. Torque predicted with dynamic simulation exhibiting no tendency of shudder for neither OilM – N to the left, nor OilM blended with 6% distilled water to the right, both simulations at 30 °C initial contact temperature.

6.1.2 Established Shudder Limit in WCTR

The results from the shudder onset investigation are shown below. In Figure 48, the controlled parameters axial load and motor speed are shown during an experiment using OilB which produced shudder. It can be seen that at the 10 second mark, fluctuations are registered in the axial load sensor.

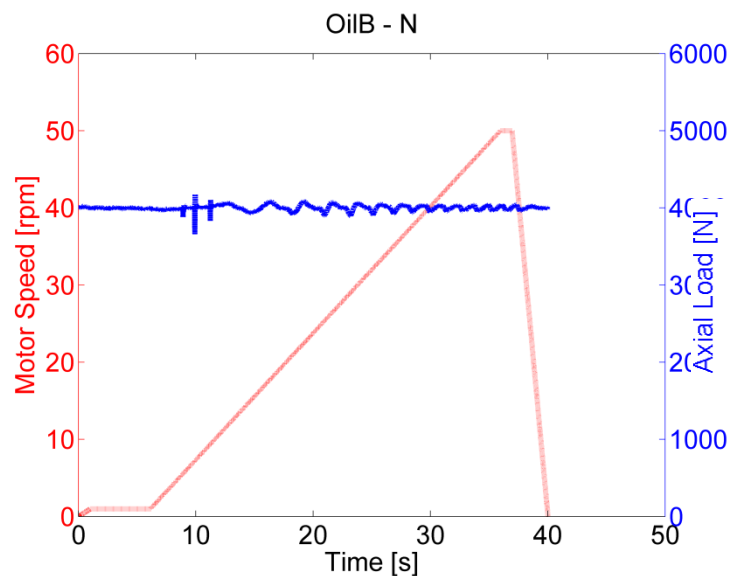


Figure 48. Motor speed and applied load in the wet clutch test rig during experiment with OilB - N.

Shudder was detected from around 10 to 25 seconds for pure OilB, as seen to the left of Figure 49 for three consecutive tests. In the right part of Figure 49, the shudder can be seen to decrease when adding fully formulated oil to OilB. For the blended oil, shudder was only registered at lower initial test temperatures. During the test cycle the contact temperature increases by around 15 °C, so shudder occurs at temperatures slightly above the initial temperature.

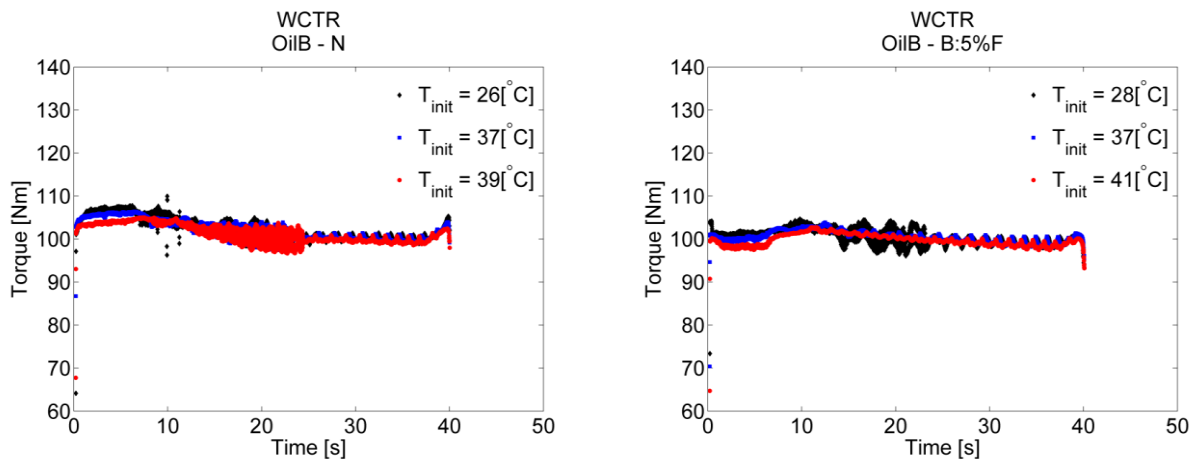


Figure 49. Measured torque in WCTR exhibiting shudder for OilB - N for three consecutive speed ramps, and for the first speed ramp with low initial temperature when using OilB blended with 5% OilF.

When using the model oil instead of the base oil, no shudder was detected, and as seen in Figure 50, adding water to OilM certainly affects the overall torque transfer but it does not produce shudder in the investigated friction system. The torque during the down-ramp is actually smoother when using OilM blended with distilled water compared to pure OilM. There is however some fluctuation seen at 10-12 seconds at 33 °C initial temperature with the water contaminated sample, which did not appear with pure OilM, but this did not produce any audible noise and is not characterized as shudder.

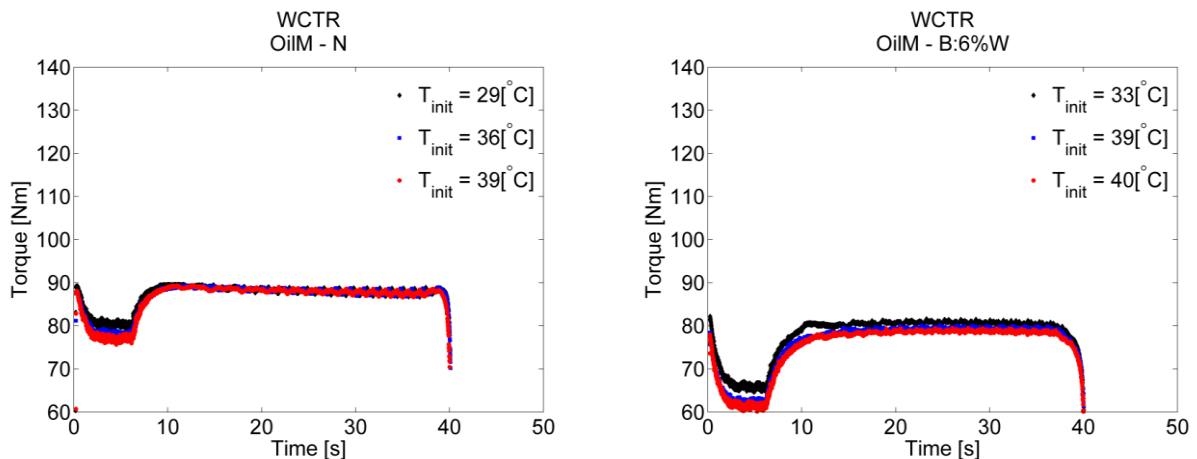


Figure 50. Measured torque in WCTR exhibiting no shudder for pure OilM to the left, and for OilM blended with 6% distilled water to the right.

Even though adding water did not produce shudder, it could negatively affect the system in other ways, and especially in the longer term in the form of corrosion to internal parts of the system. For the friction characteristics however, it does not seem to have an immediate negative effect.

6.2 Factors Influencing Accuracy of FASTER

Scaling down a component test to a model test usually means the results are more sensitive to contaminations or unwanted affects, therefore some of these factors are investigated in this section.

6.2.1 Effect of Aligning and Condition of Pin Specimen

Figure 51 shows four test runs from the pin-on-disc which all use the same oil sample and the same materials, however the exact pin specimen differs, and most importantly, the running in state. Both

PS3 and PS1 are fully run in Pin Specimen (PS) that has been subjected to the running in procedure described in section 4.1.1. The difference in this case is that PS1 was disassembled for surface analysis prior to these test runs, whereas PS3 was never dismounted after running in. The variation in friction measurement is believed to be caused by this dismounting which means that the pin specimen must be run in again before it is correctly aligned to the mating disc specimen. Run 01 with PS1 has a significantly worse $\mu - v$ relation compared to Run 02 with the same PS. No further data is available for PS1 but it is clear that the consistency is very good for PS3 which was not disassembled; these curves are indistinguishable from each other in Figure 51.

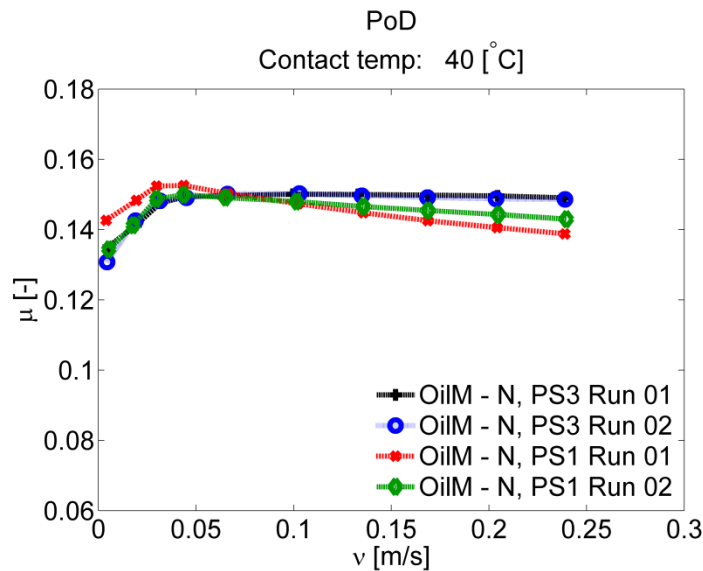


Figure 51. Friction versus sliding speed at a nominal contact temperature of 40 °C for four test runs with the same oil and materials, but different state of running in.

Images from the optical profiler of three investigated pin specimen are shown in Figure 52. To the far left is PS2 which was only used for one test cycle without running in, in the middle is PS1 prior to Run 01 in Figure 51 above, and to the far right is PS3 after Run 02.

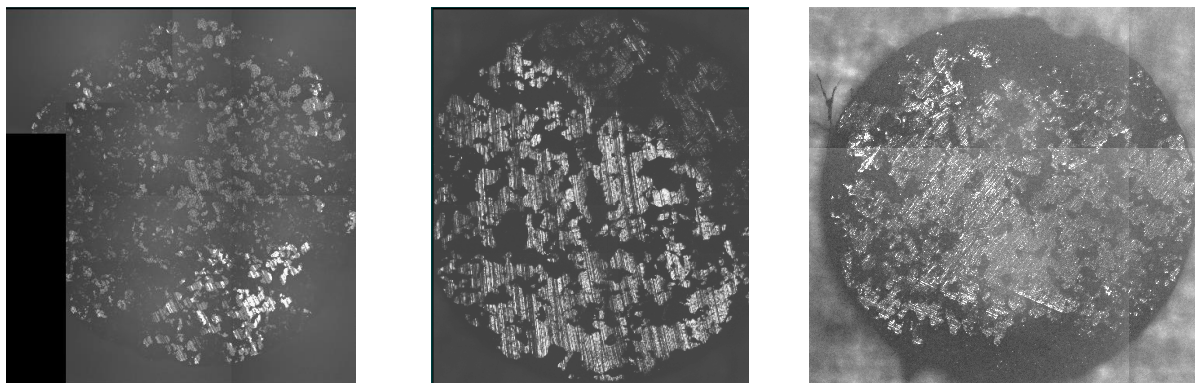


Figure 52. Different states of PS, from left to right, PS2 without run in showing a very small contact area, compared to PS1 and PS3 with approximately 75% of the nominal area being in contact.

The area subjected to contact can be seen from the bright reflective spots whereas the dark spots are pores which do not reflect any light. For PS2 seen to the left, the large roughness caused problems with measuring the surface and therefore there is a large black region in the bottom left corner. Both PS1 and PS3, seen in the middle and to the right respectively, are classified as fully run in for the purpose of this study; it can be seen however that the real area of contact is still relatively far from the nominal contact area. For these latter two PS the nominal worn area is approximately ~75% of

the nominal full area, but due to the waviness of the samples it is not possible to reach 100% nominal contact area. This variation in real area of contact will affect the contact pressure, but as shown in [25], the contact pressure is not a major factor for the friction coefficient and therefore it is not a cause of concern. The problem in Figure 51 however is likely caused by the dismounting which means that the PS must be aligned to the DS again, and before the surfaces are correctly mated to each other the real area of contact could be significantly reduced and therefore likely also affect the friction coefficient. This means that the PS not only must be run in, but it should also not be dismounted so that the aligning of the test specimen is lost.

6.2.2 Effect of Bin Distribution

Another factor which could influence the shudder prediction is the number of bins used to represent the pin-on-disc data. Figure 53 and Figure 54 shows two different bin densities used and their effect on the predicted torque. As can be seen, the effect is very small and that means that the method is fairly robust with respect to bin density. Many of the measured oil samples show fluctuations in the friction coefficient at low sliding speeds, however, it has not been investigated in this study if these fluctuations are an actual property of the oil and materials used, or if it is just errors in the measurement or an effect of the pin-on-disc experimental equipment. If the fluctuations are considered as an artefact of the test method, they could be discarded by decreasing the bin resolution as in Figure 53, whereas if the data is trusted, a higher bin resolution such as in Figure 54 could be used to capture this behavior and study its effect on shudder tendency. As seen in Figure 54 the fluctuations captured when using higher bin density can cause slight vibrations in the torque prediction but since they only affect such a small range of the sliding speed they are not a major factor in this case.

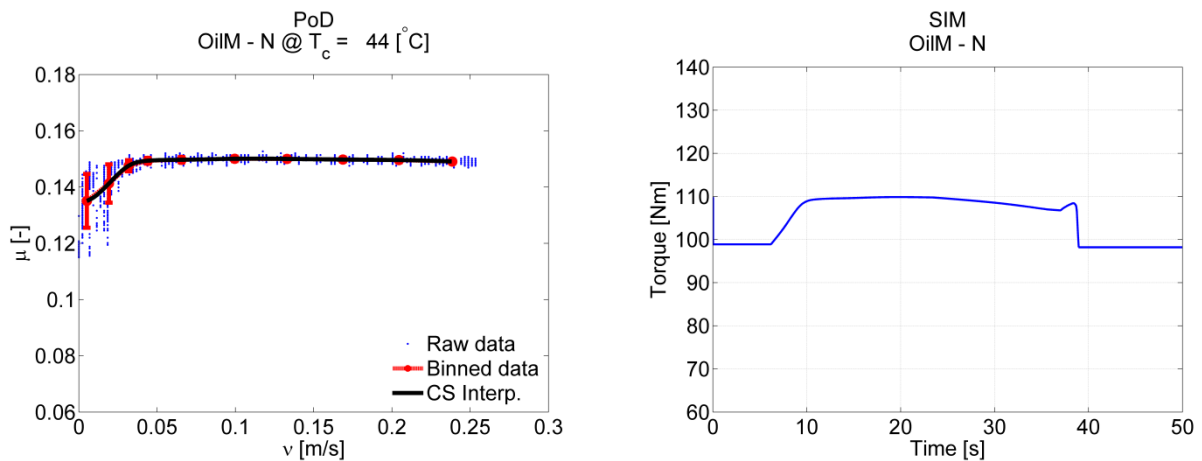


Figure 53. Low bin density gives a smoother μ - v curve and therefore also smoother predicted torque in the simulation.

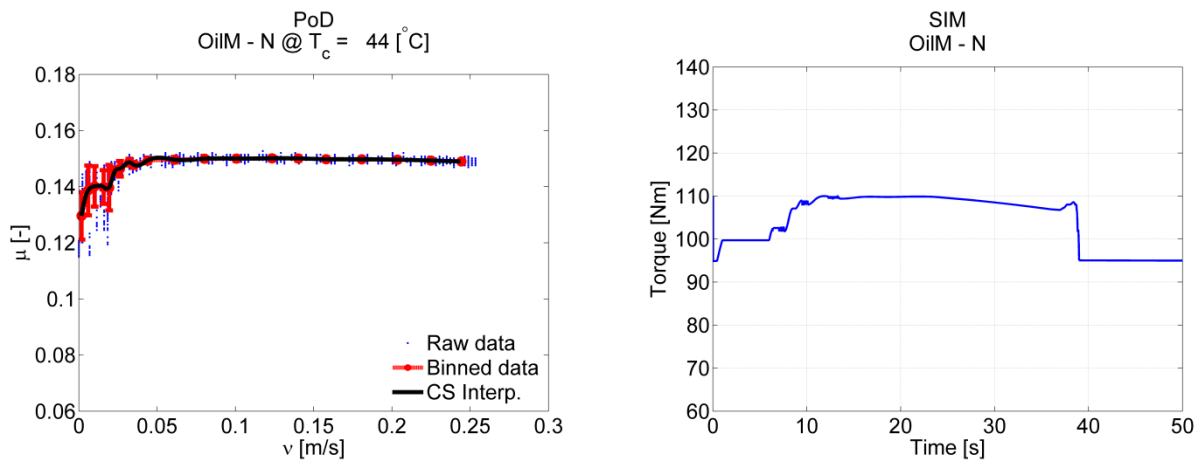


Figure 54. High bin density allows fluctuations to be represented in the μ - v curve which can affect the predicted torque in the simulation.

6.3 FASTER Prediction for Aged and Degraded Oil

In this section the results of the aged and degraded oil samples will be presented. Five oil samples were aged at 120 °C and one at 110 °C. As can be seen in Figure 55, ageing of OilM appears to initially increase friction levels, such as for the 24h aged samples, before friction levels decrease back towards the initial state. In Figure 56 which shows the friction to sliding speed relation at a higher temperature, the ageing actually improves the behavior of OilM. This is different from earlier findings when studying the ageing effects on OilF, where it has been shown that ageing produces a negative friction to sliding speed relation [5]. The cause for this behavior needs further studying but one explanation could be that breakdown of the bulk oil during oxidation produces fatty acids which act as friction modifiers. Since OilM does not contain anti-oxidants it is possible that even 24 hours at 110 °C is a very severe ageing and that the results would be different if aged at a lower temperature. The relative differences are also small for all the aged samples, so more measurements are required before drawing any conclusions.

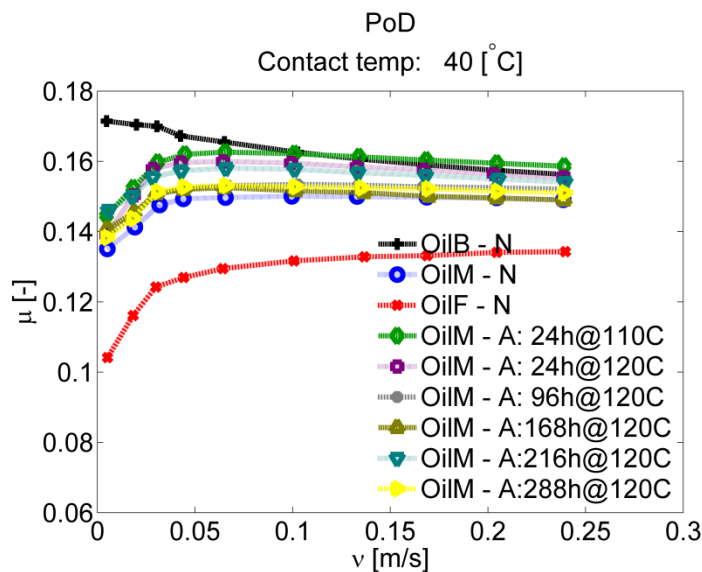


Figure 55. Friction versus sliding speed at a nominal contact temperature of 40 °C for the six aged oil samples compared to the three reference samples.

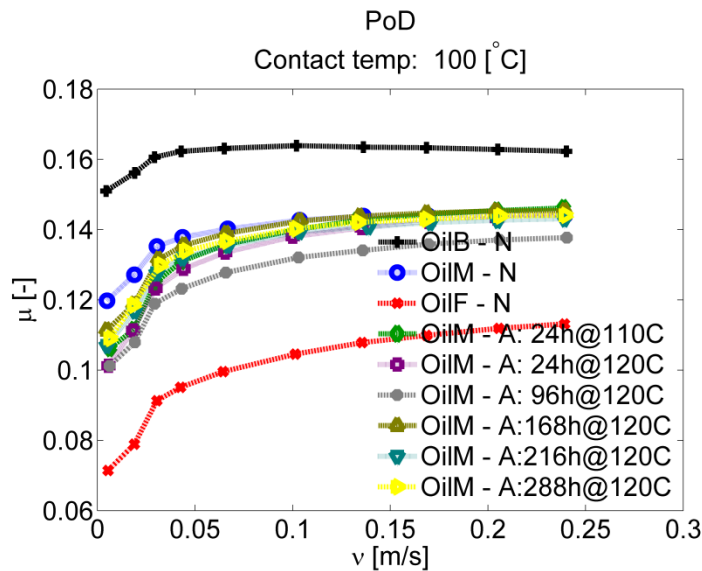


Figure 56. Friction versus sliding speed at a nominal contact temperature of 100 °C for the six aged oil samples compared to the three reference samples.

When evaluating these aged samples in the dynamic model, none of them cause shudder, as seen in Figure 57 below. For the Oil sample subjected to the mildest ageing, 24h at 110°C, there is a minimal tendency of shudder at 38 seconds in, but it is hardly even distinguishable and is not likely to be detected as shudder in the investigated friction system. None of the other aged samples causes even a slight disturbance so ageing of this model oil does not appear to cause shudder in the wet clutch system investigated.

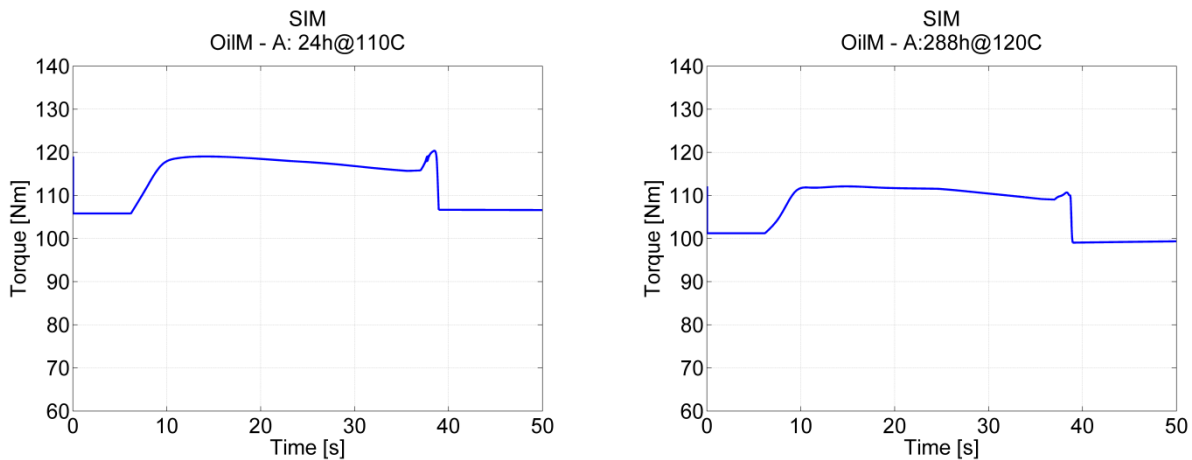


Figure 57. Torque predicted with dynamic simulation exhibiting minimal tendency of shudder at 38s for OilM aged for 24h at 110°C to the left, and no tendency for OilM aged for 288h at 120°C to the right, both simulations at 40 °C initial contact temperature.

The color shifting, and lack of color shifting for OilM was also interesting. It is well known that ageing and oxidation usually darkens oil samples, and this was also shown to be the case for the fully formulated oil, OilF, as seen in Figure 58. For OilM however, as seen in Figure 59, no apparent change in color is visible.

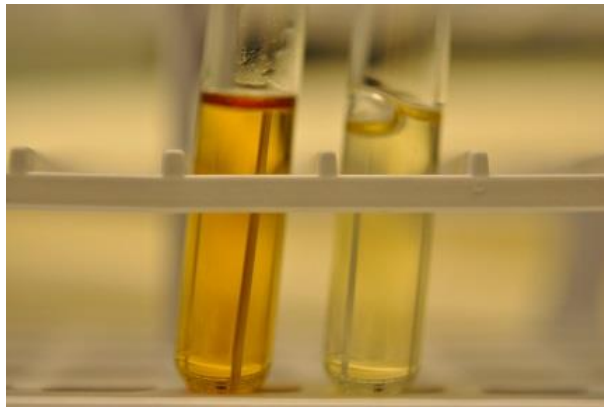


Figure 58. Color shifting in OilF, aged 168h at 120 °C to the left compared to fresh oil sample to the right.

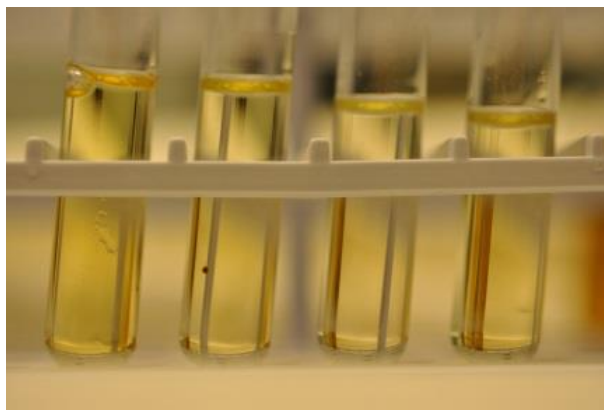


Figure 59. Minimal color shifting in OilM, from left to right, aged 288h, 168h, 24h and 0h at 120 °C.

As discussed in previous results, the main effect of degrading OilM with distilled water is lower friction. The slope of the $\mu - v$ curve is actually improved as seen in Figure 60, so from that perspective water contamination does not appear to be a major cause for concern in this system, and as seen in the dynamic simulation in Figure 61 the predicted torque is very smooth. There is however other aspects such as corrosion or effects on the hydraulic system that could be problematic with water contamination, but these factors are not detected with this test method.

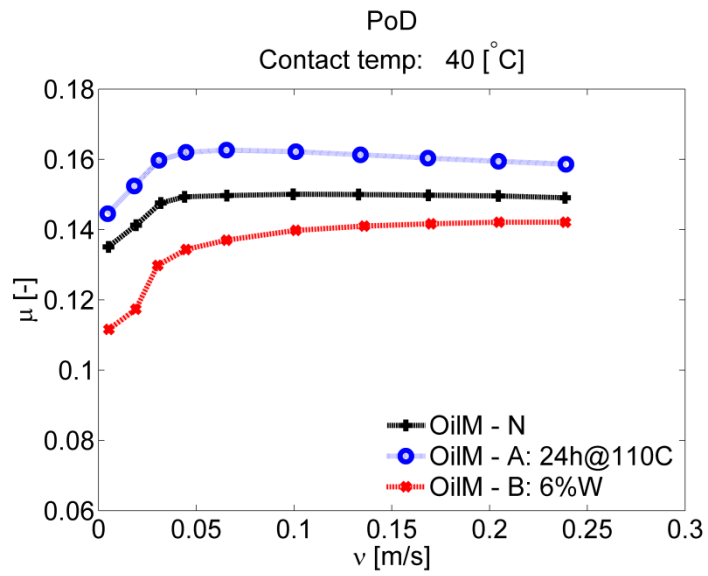


Figure 60. Friction versus sliding speed at a nominal contact temperature of 40 °C for one aged oil sample compared to the water degraded sample and a reference sample of OilM.

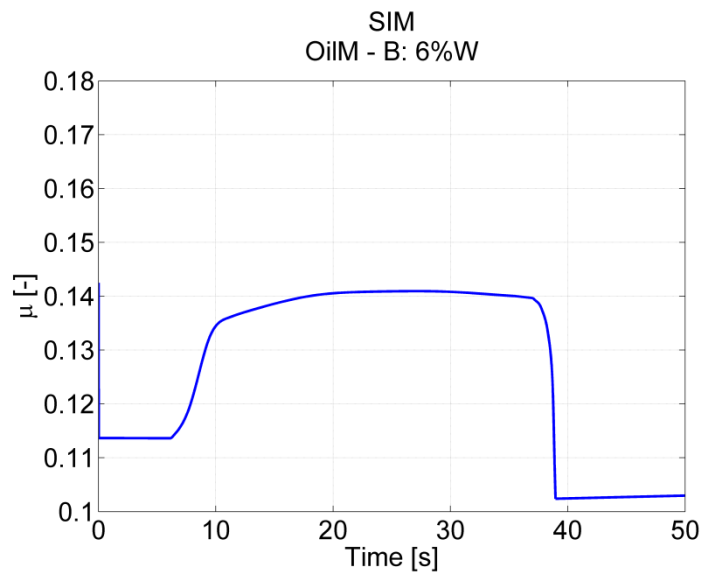


Figure 61. Torque predicted with dynamic simulation exhibiting a very smooth torque transfer for OilM blended with 6% distilled water, simulated with 40 °C initial contact temperature.

Page intentionally left blank

7 Conclusions

The main conclusion of this work is that pin-on-disc model testing in combination with the efficient data processing and analysis routine developed in this work is a very useful tool when quickly screening large amounts of oil and material combinations. Using this method, the friction data can be completely arbitrary and no assumptions are required, therefore it is well suited for analyzing completely new oil and material combinations where no prior assumptions can be made of the $\mu - v - T$ relation.

The ageing procedure still requires more work to fully understand how artificial ageing relates to ageing in the real application, and the evaluation method described in this master's thesis could likely be useful in continuing that work.

The sensitivity to contaminations and alignment errors is a factor that has to be considered when using this method; however, contaminants are always a factor and in component test rigs the cleaning procedure is often more difficult and time consuming. The alignment and running in effects of this method is something that must be kept in mind though, but a consistent running in procedure seems to produce reliable results.

Page intentionally left blank

8 Future Work

As stated in the conclusions of this work, this method should be well suited to perform quick screening tests of various oil samples, so this would be a natural continuation for future work. By enabling the possibility of these simplified screening tests, artificial ageing procedures could possibly be improved and evaluated.

To further improve this method, the accuracy of both pin-on-disc measurements and dynamic simulation can be improved. Major improvements to the PoD include;

- Finer caliber load cell, 0-5 N instead of 0-50 N
- Lower gearing of the drive motor to decrease speed fluctuations at low rpm
- Reliability issues related to the heated oil circulation system.

Further improvements would be to modify the PS holder to avoid the risk of interference from hydrodynamic effects if the holder is in contact with the oil film. A ventilated cabinet for the PoD would also be an improvement, and external cooling to the PoD would reduce downtime between experiments and enable the possibility of measuring friction below room temperature.

Regarding the dynamic simulation, the accuracy could be improved by further investigating how to model the system damping. The current damping model is a simple linear damping, but in reality it is likely non-linear and dependent on the viscosity. This could be improved by taking into account the backlash in the spline coupling. As seen in Figure 62, there is a gap in the splines which connect the clutch discs to the clutch drum. Splines are known to be a cause of non-linear stiffness and damping effects and there are techniques available to model this that could likely improve the accuracy of the model.

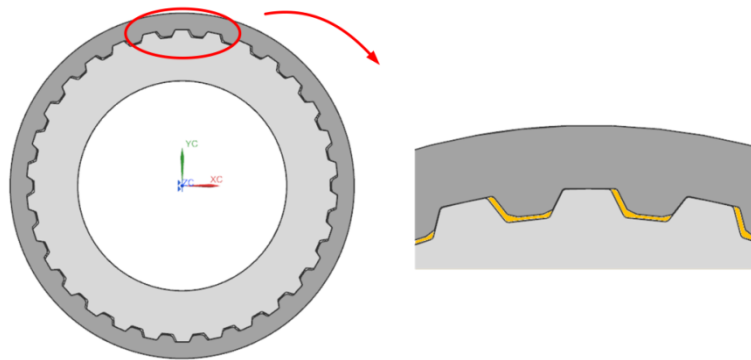


Figure 62. Gap in spline coupling which cause backlash.

Page intentionally left blank

9 References

- [1] *All-Wheel Drive: Technology Inspiring Confidence; from a Global Leader in Drivetrain Technology*. BorgWarner, 2009.
- [2] Swärd, L. (2014, March 24). Fler vill ha fyrhjulsdrift trots ökade utsläpp. *Dagens Nyheter*. Retrieved 2015-02-05 from <http://www.dn.se/motor/fler-vill-ha-fyrhjulsdrift-trots-okade-utslapp/>
- [3] Marklund, P. (2008). *Wet clutch tribological performance optimization methods*. Luleå: Luleå tekniska universitet. (Doctoral thesis / Luleå University of Technology).
- [4] Berglund, K. (2013). *Predicting wet clutch service life performance*. Luleå: Luleå tekniska universitet. (Doctoral thesis / Luleå University of Technology).
- [5] Berglund, K., Marklund, P., & Larsson, R. (2010). Lubricant ageing effects on the friction characteristics of wet clutches. Proceedings of the Institution of Mechanical Engineers, Part J: *Journal of Engineering Tribology*, 224(7), 639-647.
- [6] Berglund, K., Marklund, P., Larsson, R., & Olsson, R. (2015). Predicting Boundary Friction of Aging Limited Slip Differentials. *Journal of Tribology*, 137(1), 012101.
- [7] Marklund, P., & Larsson, R. (2008). Wet clutch friction characteristics obtained from simplified pin on disc test. *Tribology International*, 41(9), 824-830.
- [8] Bowden, F. P., & Young, J. E. (1951). Friction of clean metals and the influence of adsorbed films. Proceedings of the Royal Society of London. Series A. Mathematical and *Physical Sciences*, 208(1094), 311-325.
- [9] Bowden, F. P., & Tabor, D. (1950). *The Friction and Lubrication of Solids-Part I*.
- [10] Ingram, M., Spikes, H., Noles, J., & Watts, R. (2010). Contact properties of a wet clutch friction material. *Tribology International*, 43(4), 815-821.
- [11] Marklund, P., Larsson, R., & Lundström, T. S. (2008). Permeability of sinter bronze friction material for wet clutches. *Tribology Transactions*, 51(3), 303-309.
- [12] Ingram, M., Noles, J., Watts, R., Harris, S., & Spikes, H. A. (2010). Frictional properties of automatic transmission fluids: Part I—Measurement of friction—sliding speed behavior. *Tribology Transactions*, 54(1), 145-153.
- [13] Brown, M., Fotheringham, J. D., Hoyes, T. J., Mortier, R. M., Orszulik, S. T., Randles, S. J., & Stroud, P. M. (2010). *Chemistry and technology of lubricants*.
- [14] Ingram, M., Noles, J., Watts, R., Harris, S., & Spikes, H. A. (2010). Frictional properties of automatic transmission fluids: part II—origins of friction—sliding speed behavior. *Tribology Transactions*, 54(1), 154-167.
- [15] Fatima, N. (2014). *Impact of water contamination and system design on wet clutch tribological performance*. Luleå tekniska universitet. (Doctoral thesis / Luleå University of Technology).
- [16] Torbacke, M., Kassman Rudolph, Å., & Kassfeldt, E. (2012). *Lubricants—Properties and Performance*. Universitetsstryckeriet, Luleå.

- [17] Wang, Q., & Chung, Y. W. (Eds.). (2013). *Encyclopedia of Tribology* (pp. 3730). New York: Springer.
- [18] Gong, T., Yao, P., Xiao, Y., Fan, K., Tan, H., Zhang, Z., ... & Deng, M. (2015). Wear map for a copper-based friction clutch material under oil lubrication. *Wear*, 328, 270-276.
- [19] Marklund, P., Berglund, K., & Larsson, R. (2008). The influence on boundary friction of the permeability of sintered bronze. *Tribology Letters*, 31(1), 1-8.
- [20] Mang, T. (Ed.). (2014). *Encyclopedia of Lubricants and Lubrication*. Springer Berlin.
- [21] Popov, V. (2010). *Contact mechanics and friction: physical principles and applications*. Springer Science & Business Media.
- [22] Sheng, G. (2007). *Friction-induced vibrations and sound: principles and applications*. CRC press.
- [23] Van Beek, A. (2006). *Advanced engineering design: lifetime performance and reliability* (Vol. 1).
- [24] Berglund, K., Marklund, P., Larsson, R., & Olsson, R. (2014). Evaluating lifetime performance of limited slip differentials. *Lubrication Science*, 26(3), 189-201.
- [25] Marklund, P., Mäki, R., Larsson, R., Höglund, E., Khonsari, M. M., & Jang, J. (2007). Thermal influence on torque transfer of wet clutches in limited slip differential applications. *Tribology international*, 40(5), 876-884.
- [26] Zhao, H., Neville, A., Morina, A., Durham, J., & Vickerman, R. (2008). A new method to evaluate the overall anti-shudder property of automatic transmission fluids—multiple parameters spider chart evaluation. *Proceedings of the Institution of Mechanical Engineers, Part J: Journal of Engineering Tribology*, 222(3), 459-469.
- [27] Dubowsky, S., & Freudenstein, F. (1971). Dynamic Analysis of Mechanical Systems With Clearances—Part 2: Dynamic Response. *Journal of Manufacturing Science and Engineering*, 93(1), 310-316.

Appendix

Matlab Code – FAST Importer

Available upon request

Matlab Code – FAST Evaluator

Available upon request

Matlab Code – Inputs to dynamic model

Available upon request

Simulink Dynamic Model

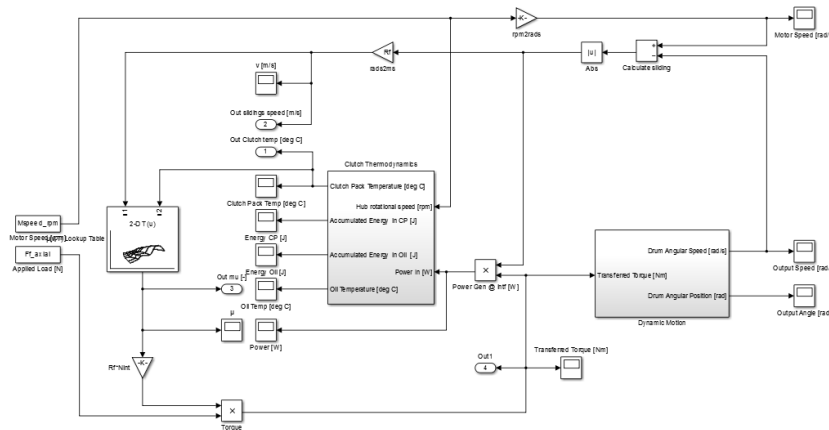


Figure 63. Overview.

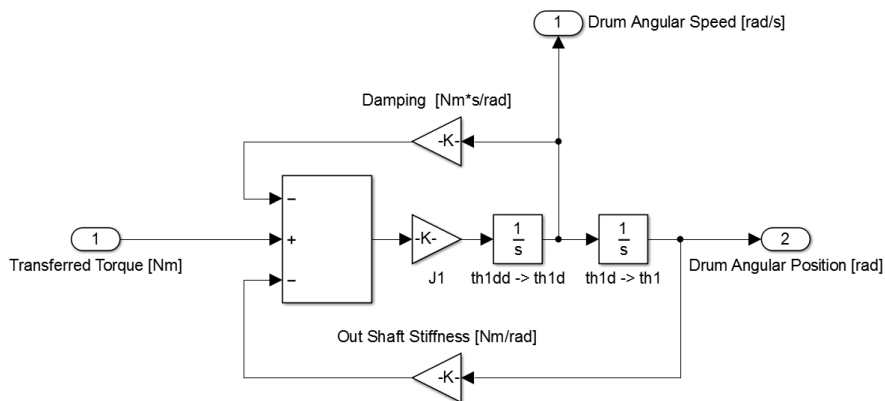


Figure 64. Dynamic Motion Sub-system.

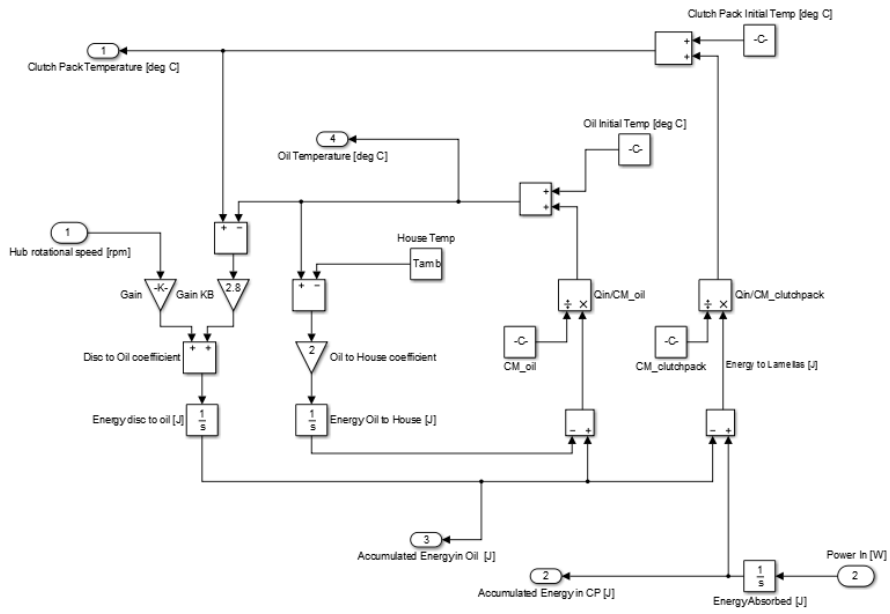


Figure 65. Thermodynamic Sub-system.